X-692-70-141
PREPRINT

NASA TM X- 63888

INTERACTION OF THE SOLAR WIND WITH THE MOON

NORMAN F. NESS

APRIL 1970

GSFC

GODDARD SPACE FLIGHT CENTER
GREENBELT, MARYLAND

X-692-70-141

Interaction of the Solar Wind with the Moon*

Norman F. Ness**

C.N.R. - University of Rome

Laboratory for Space Plasmas

April 1970

* Invited review presented at STP Leningrad Symposium May 1970.

** On leave from NASA-Goddard Space Flight Center

Laboratory for Extraterrestrial Physics
NASA/Goddard Space Flight Center
Greenbelt, Maryland 20771

Tables of Contents

Interaction of the Solar Wind with the Moon

Norman F. Ness

Abstract

During its orbit about the Earth, the Moon is located in the interplanetary medium or the geomagnetosheath-geomagneto-tail formed by the solar wind interaction with Earth. In the tail no evidence is found for a lunar magnetic field limiting the magnetic moment to 10^{20} gauss $-cm^3$. ($\sim 10^{-6}$ earth). In the interplanetary medium, no evidence exists for a bow shock or a trailing shock although a well defined plasma wake region is observed in the anti-solar wind direction. The moon absorbs the solar wind plasma which strikes its surface and creates a void region or cavity in the flow. Small perturbations of the interplanetary magnetic field magnitude (< 30 %) and direction ($< 20°$) are observed to be correlated with the location of the solar wind plasma umbra and penumbra. Characteristic perturbations in magnitude are + - + - + as a satellite transverses the wake region. The magnitude of the anomalies is correlated principally with the diamagnetic properties of the solar wind, as measured by β, and less with the direction of the interplanetary magnetic field. The observed lunar Mach cone gives evidence for the anisotropic propagation of waves in the magnetized collisionless warm solar wind plasma.

Neither the Gold-Tozer-Wilson mechanism of accretion of field lines or the Sonett-Colburn-Hollweg mechanism of unipolar induction is significant in the interaction. The transmission

of microstructural discontinuities in the interplanetary medium past the moon show little distortion, indicating a low effective electrical conductivity ($\leq 10^{-4}$ mhos/meter) which implies a relatively cool interior ($\sim 10^{3}$ K) of the lunar body. Fluctuations of the interplanetary magnetic field upstream from the plasma wake are stimulated by the disturbed conditions in that region. The moon behaves like a cold, non-magnetic fully absorbing dielectric sphere in the solar wind flow.

1.0 Introduction

The interaction of the solar wind with the Moon is a vastly different phenomenon than that of its interaction with the Earth (or the planet Venus). This is principally due to the lack of a sufficiently strong intrinsic lunar magnetic field (or ionosphere) to deflect the solar plasma flow. No bow shock wave or sheath layer of thermalized or shocked solar plasma exists surrounding the Moon. The surface of the Moon absorbs and neutralizes the charged particle and plasma flux impacting its surface and leads to the formation of a plasma cavity and wake region trailing behind the Moon for several lunar radii. The interplanetary magnetic field is at times slightly perturbed in magnitude (< 30 %) but little in direction within and near the solar wind wake ($< 20°$), depending entirely upon the characteristics of the magnetized, warm anisotropic solar plasma. The Moon behaves much like a non-magnetic, non-electrically conducting, dielectric, fully absorbent spherical obstacle in the solar wind flow.

This paper presents a review of the current state of experimental and theoretical studies of the interaction of the solar wind with the Moon. Essentially data from one lunar orbiting satellite, the U.S.A. Explorer 35, placed in orbit in July 1967 has provided all the results and interpretations upon which this understanding is based. In order to place the contemporary views in the proper context, a review of earlier satellite studies directly related to the subject of this paper is also included. The reader interested in the long studied problem of possible lunar effects in terrestrial magnetic field variations is referred to the

recent review by Schneider (1967). There, the numerous studies of the correlation between lunar phase and the planetary magnetic activity indices K_p and C_i are summarized. Those statistical research efforts did not contribute significantly to our present understanding, being due to the weak interaction which in fact occurs between the solar wind and the Moon, and the small size of the Moon when compared to the Earth's magnetosphere and tail. Attempts to simulate the problem in the laboratory are discussed by Fahleson (1967).

Observations of the solar wind interaction with the Moon are possible only during that part of the lunar synodic month when the Moon is outside the geomagnetotail and magnetosheath. This normally occurs for about $\pm$ 10 days relative to new Moon, depending upon the motion and position of the Earth's bow shock. It is possible to observe the interaction of the thermalized solar plasma with the Moon for an additional 6 days when the Moon is located within the earth's magnetosheath. For the remaining 3.5 days, the Moon is located within the geomagnetotail and occasionally imbedded within the plasma sheet associated with the field reversal region of the tail. When located within the tail the Moon is shielded from the solar wind and it is possible to measure most effectively the magnetostatic properties of the lunar body. That there are four characteristic environments of magnetized plasma for the Moon has been recognized only since 1964, following the initial studies of the solar wind interaction with the Earth.

Because of the lack of a bow shock wave, such as a strong interaction generates, and the lack of an appreciable

atmosphere, the flow of the magnetized solar plasma past the Moon depends upon the electrodynamic properties of its interior and the coupling between its surface and the adjacent plasma. Preliminary attempts have been made to deduce the electrical conductivity from the presence or absence of certain features in the characteristics of the solar wind flow. The results suggest a moderately low value of 10^{-4} mhos/meter or less for the deeper interior and much less for the near surface layers. In spite of the remarkable increase in our understanding of the topic of this review in the past 3 years, there are unresolved problems in the interpretations of the experimental data.

This paper begins with an historical review of early studies, from 1959-1966, in the satellite era. Next a discussion of the experimental findings by Lunar Explorer 35 are presented with their interpretations. Then the present status of studies of the electrical conductivity of the interior of the Moon is discussed. The paper concludes with a summary of our present understanding and problems for future studies.

2.0 Early Studies: 1959 - 1967

The first direct observational measurements related to the solar wind interaction with the Moon were those performed by the USSR lunar impacting probe Luna 2 in 1959. Subsequently in 1963-1964 the earth-orbiting IMP-1 (Explorer 18) satellite reported possible observations of the distant lunar wake. The first spacecraft placed into lunar orbit, the USSR Luna 10, provided intermittent measurements of the magnetic field and low energy plasma for a period of two months in 1966. None of these experimental studies were either sufficiently sensitive nor accurate to reveal the true nature of the solar wind interaction with the Moon. During the period 1964-1967, several theoretical studies were made of this problem. While covering a wide range of possibilities, most of them were not correct in their anticipation of the characteristics of the interaction. This section will briefly summarize these early satellite studies and also the early theoretical models proposed.

2.1 Luna 2: 1959

The USSR launched two probes in 1959 which were designed to study the Moon: Luna 1, on 2 January and Luna 2 on 12 September. Both spacecraft carried a three component magnetometer but the only lunar related results were reported from Luna 2, which impacted on the surface on 13 September 1959. (Luna 1 achieved a fly by of the Moon on 3 January at 7000 Km distance).According to the Luna 2 magnetic field studies, the Moon did not possess a magnetic field larger than 100 γ on the basis of measurements made up to 50 Km from

its surface (Dolginov et al., 1961). The errors associated with the instrumentation and the spacecraft magnetic field limited the accuracy to approximately 50-100 γ (Dolginov et al., 1960). While this result indicated that the moon possessed a much weaker intrinsic magnetic field than the Earth, it was pointed out by Neugebauer (1960) that if the solar wind compressed the lunar field then it could in fact be much stronger.

At the time these measurements were performed, the general problem of the solar wind interaction with the Earth was not understood and so the advantage of a comparative analysis could not be enjoyed. We now know that a lunar surface field of 50 γ is more than sufficient to deflect the solar wind and lead to the formation of a detached bow shock wave. But in 1959, these problems were only beginning to be defined. The absence of a stronger lunar field than the limit set by Luna 2 was not surprising due to the very low rotation rate of the Moon and its low average density. This precludes an appreciable core and a dynamo mechanism similar to the Earth which could develop and generate a lunar field.

The magnitude of the transverse magnetic field B_T that is sufficient to deflect the solar wind flow is determined by equating the directed pressure of the solar wind stream of density n and velocity V_{sw} to that of the magnetic field

$$\frac{(2B_T)^2}{8\pi} = k n m_p V_{sw}^2 \cos^2\phi \qquad (2.1.1)$$

where m_p represents the mass of the proton, the principal constituent of the solar wind. The factor of 2 in the left hand side of equation (2.1.1) is due to the induced electrical currents which arise as the magnetic field separately deflects the ions and electrons in opposite directions. The factor k is theoretically 2 for perfect reflection of the plasma from the boundary surface (which is assumed to be oriented with its normal at an angle of ϕ to the solar wind). Our present understanding of the solar wind interaction with the Earth indicates that $k = 0.88$ is a better value (Spreiter and Alksne, 1969) to employ which indicates the deflection is around an obstacle more than reflection from it. With our present knowledge of solar wind properties, assuming a density of $10/cm^3$ and a velocity of 400 Km/sec, leads to B_T of approximately 30γ for $\phi = 0°$, i.e. normal incidence.

Neugebauer (1960) used higher estimates of $n = 1000/cm^3$ and $V_{sw} = 500$ Km/sec consistent with the then contemporary views of the solar corpuscular flux. A more significant aspect, however, was that the existence of the Earth's bow shock wave had been neither predicted nor measured in 1959-1960. Thus the most important feature of the Luna 2 data, the absence of a lunar bow shock, was not considered in the interpretation of the results. Had it been, then the upper limit of the intrinsic lunar field could in fact have been set much lower.

A final point to consider in this review of the Luna 2 measurements is that of the phase or position of the Moon at the time the measurements were made. The Sun-Earth-Moon

angle was 140° East and thus it is probable that the Moon was located within the Earth's magnetosheath rather than the interplanetary medium. However, the errors in the Luna 2 measurements were so large that further consideration of this uncertainty is not meaningful.

2.2 IMP-1 (Explorer 18)

During November 1963 to February 1964, the USA spacecraft IMP-1 periodically measured the interplanetary medium from its highly eccentric earth orbit. The synchronism and geometry of its orbit were such that in December 1963 and January and February 1964 apogee was located near the extension of the Sun-Moon line. Ness et al.(1964) suggested that an observed interval of enhanced and disturbed interplanetary magnetic field during the period December 13-15 might have been due to passage of IMP-1 through the lunar wake since the satellite was favorably positioned at a distance of 150 R_M (1 R_M=1738 Km) to lie within the solar wind interaction region. A subsequent study of the data during the January and February opportunities did not yield substantiating evidence for a similar disturbance (Ness, 1965a). However, the satellite was not favorably positioned in January and in February was much more distant from the Moon at 200 R_M.

The interpretation of a lunar wake thus suggested the existence of a lunar bow shock wave and an intrinsic magnetic field. Several authors questioned the interpretation of the observed disturbance as being due to the solar wind interaction

with the Moon. Greenstadt (1965) suggested that a small solar flare, which occurred before the IMP-1 observations, might have been responsible for the disturbed conditions. Hirshberg (1966) offered the alternative explanation that the disturbance was one of a continuing series of M-Region disturbances. Ivanov (1965) postulated that the disturbance might even have been due to the solar wind interaction with the Earth and associated with disturbances propagating upstream from the Earth. Ness (1965b, 1966a and 1966b) replied to these comments and in the case of Ivanov's suggestion showed that the flow of solar wind was sufficiently super-Alfvénic to eliminate the Earth's interaction as the source. Michel (1965) examined the positions of the Moon and IMP-1 and found support for the conclusion that conditions were favorable for IMP-1's passage through the Mach cone bounding the lunar wake.

With our present knowledge of the solar wind interaction with the Moon, it appears certain that the lunar association ascribed to the IMP-1 data was incorrect and that the disturbance was indigenous to the solar wind. Whether the source was a solar flare or an M-Region disturbance has not been determined.

2.3 Theoretical Studies: 1964-1967

As the continual flow of the magnetized solar wind came to be recognized as a permanent phenomenon in interplanetary space, studies of its interaction with the Moon and its atmosphere were begun (See Figure 1). Michel (1964) initially suggested that the solar wind flow past the Moon would have characteristics somewhere between the limits of:

(1) Undeviated flow, with the solar wind being completely absorbed and neutralized upon impacting the lunar surface (See Figure 1a) and

(2) Potential flow, in which the plasma flow would be deflected around the Moon, due to an induced magnetic field as the magnetic field is "dragged past" a finite conducting lunar interior. The development of a bow shock would lead to subsonic flow behind it as shown in Figure 1b.

The principal effect of the interplanetary magnetic field was considered to be the increased cross-sectional area that would result from the finite Larmor radii for the solar wind ions. Since the major topic of Michel's study was the lunar atmosphere, and because so little was known at that time about the solar wind and its interactions, he did not develop furthur these two limiting models for the interaction.

In another study of the interaction, Gold (1966) suggested that due to the high internal electrical conductivity of the Moon, σ, the interplanetary magnetic field lines would be "hung up" in the lunar interior. This would be due to the very long diffusion times (Cowling $\tau_D = \mu\sigma L^2$) of the magnetic field when compared to the time for convection of the solar wind past the Moon ($\tau_c = 2R_M/V_{sw}$). Gold (1966) postulated the existence of a detached bow shock wave and a lunar magnetosheath since he assumed that the conductivity was sufficiently high to cause accretion of the interplanetary magnetic field.

The mechanism of Gold (1966) for the formation of a lunar

bow shock, pseudo-magnetosphere and tail was re-examined by Tozer and Wilson (1967). They noted that the electrical conductivity estimates for the Moon which Gold had used were unreasonably high. Employing lower estimates, based upon a comparison with the Earth's mantle, they concluded that only a small internal core would be sufficiently conducting to entrap the interplanetary magnetic field, due mainly to the higher temperatures in the core. As a result, no detached bow shock would develop, but only an attached shock, tangent to the surface of the Moon, as show in Figure 1c. They still envisaged the development of an accreted magnetic field and pseudo-magnetosphere.

Present understanding of the solar wind interaction indicates that of these early theoretical models, the one most closely approximating the actual flow characteristics is that of undeviated flow, one of Michel's two 1964 alternatives.

2.4 Luna 10

On 2 April 1966, the USSR placed the Luna 10 spacecraft into a close lunar orbit with perisélene =350 Km, aposolene = 1017 Km and period=3 hours. The data transmission of magnetic field, plasma and energetic particle measurements was intermittent due to limited battery life and no solar array but the measurements were distributed over a time interval of 36 days. The results from the plasma detector were interpreted as indicating the presence of the geomagnetic tail for measurements taken near full Moon (Gringauz et al., 1966). But there were no reports of a variation with Sun-Moon-Probe angle of the detected fluxes, regardless of the phase

of the Moon. The decrease in the low energy electron flux near full moon when compared to measurements in interplanetary space was interpreted to mean the presence of the geomagnetic tail.

The results from the magnetic field experiment (Zhuzgov et al., 1966) were interpreted in terms of a permanent lunar pseudo-magnetosphere which was carried along with the Moon throughout its entire orbit. In spite of uncertainties in the accuracy of the measurements of 10 γ , the interpretation given was that the relatively constant magnitudes of the fields parallel and perpendicular to the spin axis of the spacecraft were several times larger than this and also therefore much larger than the typical interplanetary field of 6 γ . Since no on-board aspect system provided directional data, a study of the orientation of the observed field was not possible. These large, steady fields were interpreted on the basis of Gold's (1966) suggestion of a trapped interplanetary magnetic field.

A question was raised by Ness (1967) regarding the interpretation of a pseudo-magnetosphere and the failure of the magnetic field experiment to observe the geomagnetic tail. This was because simultaneous measurements by IMP-3 (Explorer 28) in April and May 1966 showed conclusively that the tail extended essentially uniformly from the Earth to 38 R_E, two-thirds of the distance to the Moon ($\sim$60 R_E).

Based on a study of the position of the Moon in the geomagnetic tail region, Ness (1967) showed that it was plausible to assume that Luna 10 was located in the plasma sheet of the tail at the times of measurements. Hence it was not sensitive to the magnetic field of the tail. Dolginov

et al. (1967) reviewed their earlier interpretations and agreed with this view point but maintained the existence of a lunar pseudo-magnetosphere. It was shortly afterwards that the USA launched the Explorer 35 successfully into lunar orbit, and those results will be discussed in the next section. They show that there is never a pseudo-magnetosphere and thus it can only be concluded that erroneous zero level-corrections and spacecraft fields contributed to the incorrect interpretations of Luna 10 data.

3.0 Recent Studies: 1967 - present.

The USA spacecraft Explorer 35, placed into lunar orbit on 22 July 1967, provided the first accurate measurements of the nature of the solar wind interaction with the Moon. The 104 Kg. magnetically clean spin stabilized spacecraft was the second in a special set of two modified satellites of the IMP (Interplanetary Monitoring Platform) series. Known as IMP-D and E before launch, they included a 4^{th} stage solid propellant retromotor for injection into a captured lunar orbit. The first attempt on 1 July 1966 failed and Explorer 33 achieved instead a highly eccentric earth orbit with apogee greater than 80 R_E (1 R_E = 6378 Km).

The second launch on 19 July 1967 was successful and Explorer 35 was injected into a very stable lunar orbit with period 11.5 hours, inclination = 169°, aposelene = 9388 $\pm$ 100 Km (5.4 R_M) and perisélene = 2568 $\pm$ 100 Km. (1.4 R_M). The principal perturbation consists of a fortnighty modulation of the semi-major axis of the orbit due to the gravitational masses of the Earth and Sun. As the Earth-Moon system orbits the Sun, the aposelene-moon-sun angle changes annually by $>360°$ so that the entire region of solar wind interaction from perise-lene to aposelene is sampled throughout the year. The space-craft carried magnetometers, energetic particle detectors and plasma probes which have functioned continuously since launch during more than 2100 orbits and data has been received continuously except for occultation periods when the body of the Moon blocks Earth reception. The spin axis of the space-craft is normal to the ecliptic ($\pm$ 2°) and the spin rate is 25.6 $\pm$ 0.4 rpm. An earlier review (Ness, 1969) briefly summa-

rized the scientific results from all of the experiments on Explorer 35 up through May 1968. The present paper extends the review of Explorer 35 data through April 1970, although from only the magnetometers, plasma probe and energetic particle detectors. In addition a review of relevant theoretical studies is included.

3.1 Early Magnetic Field-Plasma Results: Explorer 35

Preliminary reports on the NASA-GSFC magnetic field experiment (Ness et al., 1967) and the MIT plasma probe (Lyon et al., 1967) were presented at the NASA Santa Cruz Summer Study on Lunar Exploration held in August-September 1967. These results showed

1. The absence of a lunar magnetic field greater than 2 gamma at satellite periselene when the Moon was in the geomagnetic tail,
2. The absence of a bow shock wave or magnetosheath (similar to the Earth's) surrounding the Moon, when it was in the interplanetary medium (See Figure 2a) and
3. The existence of a plasma cavity or void region behind the Moon when in the solar wind flow (See Figure 3).

The first results indicated that the Moon did not possess a dipole moment greater than 4×10^{20} cgs units ($M_E = 8 \times 10^{25}$ cgs) so that no deflection of the solar wind would occur when the Moon was in the geomagnetosheath or solar wind flow (See also Sonett et al., 1967). No significant disturbance of the magnitude of the magnetic field was noted as the spacecraft passed through the downstream region of solar wind flow past the Moon.

The only effect noted in the interplanetary field was the existence, sometimes, of:

4. Field magnitude increase in the region corresponding to the plasma umbra and
5. Field magnitude decreases on either side, in the plasma penumbra.

These anomalies were interpreted in terms of the diamagnetic properties of the solar plasma (See also Colburn et al., 1967).

The absence of a pseudo-magnetosphere was interpreted by Ness et al. (1967) to mean that the effective electrical conductivity of the Moon was quite low, less than 10^{-5} mhos/meter, and that the Moon did not entrap the interplanetary magnetic field as suggested earlier by Gold (1966) and Tozer and Wilson (1967). The results also indicated that there existed no detached bow shock as suggested in one of Michel's 1964 models (See Figure 1b) nor a shock tangent to the lunar surface as suggested by Tozer and Wilson (See Figure 1c)

The determination of the topology of the magnetic field in what is now called the Lunar Wake region was complicated by the spacecraft spin rate behavior when located in the optical shadow of the Moon. Although the spacecraft provided a pseudo-Sun reference signal when in shadow, based upon the last measured spin period when illuminated, the spin rate of the spacecraft changed during the shadow crossing. This was due to the physical contraction of the spacecraft after removal of the solar thermal input, the associated decrease in angular moment of inertia and the concomitant increase in spin rate to conserve angular momentum. When the spacecraft reentered

sun light, the spin rate decreased to its normal pre-shadow value. The change in spin period was only 0.1 % of the normal value but since this was integrated through the shadow passes (up to 1 hour in length), the net effect was to lead to a linearly increasing angular error in the azimuthal angle ϕ_{SE} of up to more than 360° at the end of the shadow. Taylor (1968) developed an algorithm to determine the corrections to be made to the directional measurements when Explorer 35 was located within the shadow.

Using this method to rectify the magnetic field measurements, Ness et al. (1968) studied the detailed structure of the geometry and magnitude perturbations of the interplanetary magnetic field. The results showed that:

6. The field direction is only slightly perturbed ($< 20°$) in the lunar wake from that in the undisturbed solar wind (See Figure 2), and
7. Sometimes there exist increased field magnitudes in the penumbral regions in addition to the penumbral decreases and umbral increase previously noted (See Figure 2b). These magnitude perturbations are generally small (< 30 %).

In a study of simultaneous observations of the interplanetary magnetic field by Explorer 35 in the lunar wake and Explorer 33 in the undisturbed interplanetary medium, Taylor et al.(1968) showed conclusively that these perturbations were associated with the solar wind interaction with the Moon and not intrinsic to the solar wind (See Figure 4a). When the spacecraft distance was greater than 4 R_M behind the Moon, no effec

of the Moon was detected in either the magnitude, direction or rapid fluctuations as measured by the RMS deviation over an averaging interval of 81.8 seconds (See Figure 4b).

In summary, these experimental data showed that the solar wind interaction with the Moon was quite weak when compared to the Earth. The Moon appeared to behave like a spherical obstacle in the solar wind flow which absorbed the plasma flux incident on its surface but permitted the interplanetary magnetic field to be convectively carried past it without significant distortion or the formation of a pseudo-magnetosphere or shock waves. The next section discusses those theoretical studies and considerations which followed these experimental measurements.

3.2 Theoretical Studies

An investigation of the theoretical model for solar wind interaction with the Moon begins with a consideration of the physical parameters of the magnetized solar plasma at 1 A.U. relative to the size and properties of the Moon. The situation is summarized in Figure 5 for typical solar wind parameters. The definition of the symbols used is as follows:

V_{sw} = Velocity of Solar Wind
n = Number density of ions (electrical neutrality assumed)
B_o = Interplanetary Magnetic Field at angle ϕ_o to Moon-Sun line
T = Temperature (parallel, $T_{//}$, and perpendicular, $T_{\perp}$, to the magnetic field)
V_T = Thermal velocity of particles (RMS value) corresponding to T
R_L = Larmor (cyclotron) radius
τ_L = Larmor (cyclotron) period
L = Characteristic Wake Length Scale

γ = Characteristic Time Scale (required to convect past Moon)

β = Ratio of plasma pressure (perpendicular to field line) to perpendicular magnetic field pressure

V_A = Alfvén velocity.

It is seen that the Larmor Radius is small (<2 %) compared to the radius of the Moon. Thus, from a kinetic plasma viewpoint, a guiding center approximation would be valid in a first approximation since it is also known from experimental observations that the distances over which the small field magnitude and direction changes occur is large compared to the Larmor radius.

From a continuum approach, a measure of the <u>effective</u> mean free path for particle interactions determines the length scale for collective fluid-like phenomena. This may range from the Debye length ($\sim$1-10 meters) to the Coulomb collision mean free path ($\sim 10^7$ Kms). The correct value is not known exactly but the success of fluid descriptions of solar wind flow past the Earth suggest it is very much less than the size of the magnetosphere. The existence of classical MHD discontinuities in the interplanetary medium has been interpreted in terms of an interaction length scale less than the "thickness" of the thinest of these, 500 Km. (Siscoe et al., 1969). Many of the theoretical studies have assumed that a continuum-fluid description is appropriate in the analysis of the solar wind interaction with the Moon.

In either approach, there is agreement that:

1. The surface of the Moon is modeled as a perfect(or near-perfect) absorber of particle or plasma fluxes and
2. The flow of the solar wind is highly supersonic with respect to the velocity of propagation of disturbances in the medium.

Thus, item (1) assures that there can be no bow shock wave and item (2) that the region of disturbed solar wind flow will lie principally behind the Moon centered on its geometric shadow with respect to the solar wind flow velocity.

Sonett and Colburn (1967) studied the induction of a Lunar unipolar generator and the formation of an associated bow shock wave as a result of the interplanetary magnetic field being convectively transported past the Moon. They showed that the interaction with the moon could range from weak to strong, with the formation of a magnetosheath and the development of a shock wave, for values of a homogeneous interior electrical conductivity between 10^{-6} to 10^{-3} mhos/meter. No specific model for the Moon was proposed, although it was noted that a unipolar mechanism could not function for those planets with insulating mantles.

Shortly after the early results from Explorer 35 were reported (See Section 3.1), Michel (1967) proposed that as the solar wind closed in behind the Moon, a shock wave would be generated when the collapsing plasma was halted (See Figure 6a). This trailing shock was predicted on the basis of zero

magnetic field pressure in the plasma cavity and assumed that the plasma behaved purely hydrodynamically. The existence of a hypersonic rarefraction wave tangent to the lunar surface was also suggested as the plasma expanded to fill the cavity or void.

Johnson and Midgley (1968) qualitatively studied the closure of the plasma cavity including the effects of both the interplanetary magnetic field and different limiting models for the electrical conductivity of the lunar interior. In the case of a non-magnetic, non-conducting moon they showed that the flow pattern behind the moon would be confined to a region bounded by a rarefaction wave front which would have its origin at the point where the Mach cone would be tangent to the Moon, instead of at or behind the terminator with respect to solar wind flow. A decreased magnetic field was expected to occur in the region where the plasma expanded to fill the cavity, which itself would contain an increased magnetic field. The collapse of the plasma into the cavity generated both 'fast' and 'slow' magnetosonic waves and a detached trailing shock wave, depending upon the relative orientation of the interplanetary magnetic field and solar wind velocity.

For the limiting case of a moon with a perfectly conducting interior and an insulating exterior, the existence of a detached bow shock was predicted with the field lines slipping around the Moon through the outer layer as shown in Figure 7. A number of other models for the electrical conductivity were also considered but the major features of the flow pattern behind the moon were unchanged.

In an expansion of his earlier study, Michel (1968a) included the effects of the magnetic field in modifying the geometry of the previously proposed trailing shock (See Figure 6b). Regardless of the orientation of the field, a trailing shock was expected as the solar plasma collapsed to fill the cavity region. In between the rarefaction wave and the cavity, the decreased density of the expanding plasma led to a decrease of the component of the magnetic field transverse to the direction of the expansion but there was no effect on the parallel component. Within the cavity an increased magnetic field was expected due to the compression of the vacuum magnetic field by the magnetized solar plasma.

In studying the geometry of the boundaries of the rarefaction wave and plasma void, Michel (1968a) proposed that they would be elliptical in shape (See Figure 8). This is due to the difference in the propagation velocities of the magnetoacoustic, V_{MA}, and the acoustic modes, V_S. $V_{MA} = \sqrt{V_A^2 + V_S^2}$, where $V_A = \frac{B}{\sqrt{4\pi\rho}}$ is the Alfvén velocity and V_S is the acoustic velocity $= \sqrt{\frac{\gamma p}{\rho}}$. (Here ρ is density, p is pressure and γ is the ratio of specific heats). The factor C in Figure 8 is different for each velocity and is related to the parameter γ and the ratio of the total pressure inside the plasma void to the pressure outside. For nominal solar wind parameters and expansion into a vacuum, C = 3, for the acoustic mode. For expansion into a region having a pressure one-half the ambient, C = 0.4, for the magneto-acoustic mode.

Using the alternate approach of a guiding-center approximation, Whang (1968a) quantitatively studied the ion wake

of the solar wind flow in a first approximation by assuming that the directional and magnitude perturbations of the interplanetary magnetic field were negligible. Using a Maxwellian distribution of ion thermal velocities with mean value $V_{\parallel i}$ and defining the speed ratio $S_i = V_{sw}/V_{\parallel i}$, he determined the three dimensional geometry of the plasma wake as a function of the orientation of the magnetic field, ϕ_o, relative to the solar wind velocity. These results showed that the wake was confined to a region aftward of the Moon (See Figure 9a) and was not axially symmetric. The predicted properties of the ion wake were that it was:

1. Elongated to greater than a lunar diameter in the plane of symmetry defined by the magnetic field direction and solar wind velocity (the normal $\vec{n} = \vec{V}_{sw} \times \vec{B}_o$), (See Figure 9b),
2. Restricted to be exactly 1 lunar diameter thick transverse to this symmetry plane (See Figure 9b),
3. The axis of the elliptically shaped plasma cavity was slightly deviated from being parallel to the solar wind velocity vector,
4. The thermal anisotropy of the plasma increased substantially in the cavity since only those particles with high thermal speed parallel to the field could enter the cavity region and
5. The direction of plasma flow becomes markedly deviated towards the axis of the cavity within the cavity region.

The length of the wake depended upon ϕ_o, being infinitely long

when $\phi_o = 0°$ (or 180°) and shortest when $\phi_o = 90°$ (or 270°). The possibility of plasma instabilities, due to the modified distribution functions in the lunar wake, was not considered.

Using this first approximation disturbed ion wake, Whang (1968b) and Ness et al. (1968) computed the magnetic field perturbations that would arise from the electrical currents induced in the disturbed ion wake. These computations were based upon a cylindrical moon and the final field configuration, derived iteratively, satisfied Maxwell's equations consistent with the first approximation of the ion wake. These studies introduced two additional parameters into the problem; namely: the β of the plasma and η, the temperature anisotropy of ions, $T_{\parallel}/T_{\perp}$. A representive profile of the magnitude of the magnetic field is shown in Figure 10a illustrating the prediction of the umbral increase quite successfully but not the penumbral decreases of the field magnitude. In this treatment, the electrical currents induced in the lunar wake were computed from the following sources: Gradient Drift, Curvature Drift and Magnetization.

An extension of the earlier work by Michel, Johnson and Midgley using the continuum fluid approximation was made by Wolf (1968). He studied quantitatively the problem of flow past the moon, approximated by a cylinder, for the case of aligned field and flow velocity and an isotropic pressure of the magnetized plasma. He also considered qualitatively the case of the field being slightly oblique to the flow direction for a spherical Moon (See Figure 11). The conclusions

were the same as those of Michel (1968a), namely: the existence of a trailing shock wave, an umbral increase and penumbral decreases of the magnetic field magnitude.

Extending the theory of a trailing shock to very large distances behind the Moon, $>100\ R_M$, Michel (1968b) re-interpreted the earlier IMP-1 observations and interpretations (See Section 2.2). He concluded that the December 1963 data indicated the presence of too large an energy density in the magnetic field fluctuations to be caused by the lunar wake. Instead he proposed that the February 1964 observations, of very small increases in the magnetic field fluctuations, earlier interpreted as not representing the lunar wake, could indeed be due to his proposed trailing lunar shock. The observations of Taylor et al. (1968) do not support this view (See Section 3.1).

None of these theoretical studies by Michel, Johnson and Midgley, Whang or Wolf, predicted or anticipated the existence of the penumbral magnetic field increases. This feature of the magnetic field perturbations in the lunar wake was first treated by Siscoe et al. (1969) in a joint analysis of Explorer 35 plasma and magnetic field data. These authors found that the penumbral increases of the magnetic field were correlated with small increases of the plasma flux and possibly a small ($<3°$) outward deflection of the plasma flow away from the main ion wake (See Figure 12). (It should be noted that the digitization interval of the angular measurements of plasma flow direction for the experiment was 3°).

From this they deduced that the effective lunar profile for the solar wind flow past the moon included a small deflection

of the plasma at the limbs which led to the detached compression wave followed by the rarefaction wave and expansion fan. Three possible sources for the deflection were noted:

1. Magnetic pressure produced by solar wind induced electrical currents in the body of the Moon,
2. Interaction with a neutral atmosphere or
3. Increased solar wind pressure due to incomplete absorption of particles that impact the surface.

In a quantitative theoretical study of the outer wake region for a two dimensional body in the hypersonic limit, Siscoe et al. (1969) concluded that the plasma flow was deflected inward toward the wake axis and that the plasma flux increase was due to an increased plasma density, because the ratio of B/ρ was constant in the wake penumbra. Their explanation of the penumbral increases, however, required the introduction qualitatively of an ad hoc deflection mechanism at the lunar limb.

In a modified theory taking into account a 4^{th} induced current source, the acceleration drift or polarization current, Whang (1969) introduced an ad hoc positive perturbation of the magnetic field at the limbs which propagated back exterior to the rarefaction wave or lunar Mach cone. As before, a numerical solution to the two dimensional flow pattern, but now also taking into account the anisotropic propagation of disturbances, yielded a quantitative result which agreed quite closely with experimental observations (See Figure 10b). The suggestion was made that the field perturbations at the limbs was due

to the sudden change in magnetic permeability between the solar plasma and the body of the Moon.

Of all the theoretical studies conducted, only those by Whang have quantitatively taken into account the thermal anisotropy of the solar plasma and the case of arbitrary orientation of the field relative to the flow velocity. For the fluid-flow approximations, a simple polytropic relation between pressure and density was assumed. In the quantitative studies, the necessity of using a two dimensional geometry, in which the flow past a cylinder is computed, restricts the utility of the results in the real three dimensional flow past a spherical obstacle to within a few lunar radii of the Moon.

No theory for the flow characteristics past the Moon was advanced prior to the experimental studies identifying the unique features of the magnetic field perturbations. A comprehensive study of the observed characteristics of the plasma flow in the lunar wake has yet to be completed. Thus far, the model of Whang provides the best quantitative basis for predicting the characteristics of the interaction of the solar wind with the Moon.

3.3 Additional Explorer 35 Results

Subsequent to the early magnetic field and plasma observations discussed in Section 3.1, additional features of the solar wind interaction were studied as well as properties of the Moon itself. In a refined study of the magnetic properties of the Moon, Behannon (1968) lowered the upper limit for the permanent dipole moment to 10^{20}

gauss-cm^3, which corresponds to a surface field on the Moon of less than 4 gammas. Also utilizing the oppositely directed fields in the tail, he set an upper limit for the induced magnetic moment of the same value. For a homogenous Moon, whose interior is below the Curie point, this corresponds to a magnetic permeability μ less than $1.8\mu_0$.

The absorption of particles by the Moon having energies much higher than the solar wind has been studied by Lin (1968) and Van Allen and Ness (1969). For high energy, isotropic galactic cosmic rays, with Larmor radii much larger than the lunar radius, these authors showed that the Moon behaves as an absorber with the occultation of particle fluxes being directly related to the solid angle subtended by the lunar body.

For anisotropic solar electron fluxes with Larmor radii much less than the lunar radius, the Moon behaves as an occulting disk for those field lines which intersect the Moon. The computation of the impact parameter, D, measuring the distance of the field line from the center of the Moon is illustrated in Figure 13a. Using simultaneous measurements of the magnetic field and particle flux of electrons with $E_e > 45$ Kev, Van Allen and Ness (1969) showed that in the interplanetary medium and the magnetosheath there was essentially perfect agreement between predicted ($D \leq R_M$) and observed particle shadows (See Figure 13b). This was based on rectilinear extension of the field line from the spacecraft to the vicinity of the Moon. The agreement of the shadows permitted a selection to be made between the two geometries of the magnetic field shown in Figure 14. Clearly the directional

distortion, as suggested by Johnson and Midgley (See Figure 7) and shown in Figure 14a is not consistent with the correlated measurements. Thus it is concluded that the field lines must intersect the Moon in a manner similar to that shown in Figure 14b.

Ogilvie and Ness (1969) studied the relationship between the magnitude of the umbral increase observed by Explorer 35 with the ion plasma characteristics observed simultaneously by Explorer 34 in interplanetary space. They determined the observed relative field increase in the umbra as a function of the solar plasma ion β value. The increase was observed to be linearly dependent upon the β value as

$$\left.\frac{\Delta|\vec{B}|}{B_o}\right|_{umbra} \doteq (0.7 \pm 0.3)\,\beta_{i_{meas.}} \qquad 3.3.1$$

No consistent variation with field direction was detected although Whang's theory suggested that such a variation should be observed. In comparing the observed relationship, with that predicted by Whang (1968b),

$$\left.\frac{\Delta|\vec{B}|}{B_o}\right|_{umbra} \doteq (0.23 \pm 0.09)\,\beta_{i_{THEORY}} \qquad 3.3.2$$

a significant discrepancy was noted. This was interpreted to be due to the lack of explicit inclusion of the electron contribution in the theory, so that these data suggested

$$\beta_{i+e} \approx 2\beta_i$$

or that

$$\beta_e \approx 2\beta_i \qquad 3.3.3$$

in the solar wind. This use of the lunar wake as a solar wind sock to measure indirectly the electron temperature in the solar wind yielded a result in favorable agreement with direct measurements.

Small amplitude, rapid fluctuations stimulated by the lunar wake were detected by Ness and Schatten (1969). These fluctuations were observed on field lines which intersected the wake region both upstream and downstream from the wake. A sample of these fluctuations is shown in Figure 15. The relevant parameters describing the spacecraft position in seleno-centric solar ecliptic coordinates is shown as the longitude ϕ_{SSE} measured eastward of the Moon sun line and the radial distance RAD. The shaded regions on the abscissa represent times when the field line, extrapolated in a manner identical to that shown in Figure 13a, intersected a simplified lunar wake (a cylindrical region extending downstream from the Moon). The numbers above these shaded regions indicate the distance from the spacecraft to the point of closest approach to the lunar wake along the extended field line. It has been observed that the magnetic field is extremely steady and quiet in the core of the lunar wake.

It is seen that the noise occurs outside the umbral region in close coincidence to the times when the field lines thread the lunar wake. Ness and Schatten (1969) interpret these fluctuations as associated with electrons reflected from the electric field in the penumbral region of the lunar wake. Krall and Tidman (1969) present an interpretation in terms of a ballistic wake phenomenon associated with the steep

plasma density gradients in the plasma cavity boundary(the penumbra)and the occurrence of drift instabilities in such a region.

3.4 Lunar Mach Cone

In a careful study of the geometry of the penumbral increases and decreases, Whang and Ness (1970) have confirmed the elliptical geometry of the lunar Mach cone or rarefaction wave predicated by Michel (1968a) and suggested by Johnson and Midgley (1968). The method of Mach cone identification using the NASA-GSFC magnetic field data is illustrated in Figure 16. It is assumed that the change in sign of the magnetic field magnitude anomaly in the penumbra coincides with crossing of the rarefaction wave or Mach cone. When the exterior penumbral positive anomaly is not present the crossing is defined by the outer limit of the penumbral decrease. Using the spacecraft position relative to the plane of symmetry, as shown in Figure 17, it is then possible to relate the Mach angle, α, to the direction of propagation of the rarefaction wave relative to the magnetic field, ψ.

Recalling that the orbital plane is almost parallel to the ecliptic plane, permits a measurement of the aberrated solar wind flow direction. Determination of the Mach angle as a function of ψ provides the first measurements of the anisotropic propagation of magnetoacoustic waves in the solar plasma. The experimental results for $\psi = 90°$ are shown in Figure 18, where it is seen that the axis of the Mach cone is deviated by 4.5° from the Moon-Sun line. Using Explorer

35 MIT solar plasma speed measurements (H.S. Bridge and J.H. Binsack, private communication) during this time interval predicts an aberration of 4° ±.5°. The discrepancy is interpreted in terms of an azimuthal component of the solar wind velocity of 5 ± 5 Km/sec at 1 A.U. in the direction of planetary motion. This is in reasonable agreement with other methods.

The observed Mach cone angle, α, of 8° yields an MHD velocity of propagation, $V_\perp$, of 60 Km/sec since for $\psi = 90°$

$$\sin \alpha_\perp \approx \frac{V_\perp}{V_{SW}} \qquad 3.4.1$$

It is also observed that α varies with ψ, as shown in Figure 19. This shows that the velocity of propagation of magnetohydrodynamic waves parallel to the field direction, $V_{//}$, is less than $V_\perp$ since $\alpha_{//}$ is only 5.5°. Thus $V_{//}$ = 41 Km/sec and the velocity anisotropy is $V_\perp / V_{//} = 1.45 \pm 0.20$(0.5)

The velocity anisotropy using fluid flow models and assuming a magnetized fluid is given by:

$$\frac{V_{MA}}{V_S} = \sqrt{\frac{\gamma_P + B^2/4\pi}{\gamma_P}} = \sqrt{1 + \frac{2}{\gamma\beta}} \qquad 3.4.2$$

For a magnetized collisionless plasma, Lüst (1959) has shown that

$$V_\perp = \sqrt{\frac{1}{\rho}\left(2P_\perp + B^2/4\pi\right)} \qquad 3.4.3$$

$$V_{//} = \sqrt{\frac{1}{\rho}\left(P_\perp - P_{//} + B^2/4\pi\right)} \qquad 3.4.4$$

Thus, the velocity anisotropy is given for this more realistic model of the interplanetary medium as:

$$\frac{V_\perp}{V_{11}} = \sqrt{\frac{1+\beta}{1-\frac{\beta}{2}(\eta-1)}} \qquad 3.4.5$$

Using nominal values of $\beta = 1$, $\eta = 1.2$ and $\gamma = 5/3$ we obtain

$$\frac{V_{MA}}{V_S} = 1.48 \quad \text{and} \quad \frac{V_\perp}{V_{11}} = 1.49 \qquad 3.4.6$$

These are in reasonably good agreement with the observations of 1.45.The discrepancy between theory and observations can be accounted for in the fluid flow model by either increasing γ or β. For the magnetized collisionless plasma theory, a reduction of β or η is sufficient. Since the electrons are probably much more isotropic than the ions and are much hotter, they act to reduce the value of η.

It should be noted, of course, that the absolute values of the velocities depend upon the use of the supporting plasma data and assume that there are no explicit correlations between solar plasma speed and direction. This later assumption is probably not completely valid but it does not alter the interpretation of the observed velocity anisotropy of 1.45.

4.0 Lunar Electrical Conductivity

As discussed by Gold and Tozer-Wilson, the interior electrical conductivity is the principal factor determining the characteristics of the solar wind interaction with the unmagnetized atmosphereless Moon. Thus, by inverting this relationship, it should be possible to deduce characteristics of the interior electrical conductivity from the observed features of the lunar wake. Since the observations are indirectly related to the electrical conductivity, it is necessary to have a number of models of possible conductivity structure available for comparison.

The electrical conductivity of typical minerals and rocks within the Earth's mantle depends upon temperature, pressure, composition and the fluid filling the cracks, pores and interstices. At the elevated temperatures and pressures in the deep mantle, $>$ 400 Km, only the pressure, temperature and composition are important. In the case of the Moon, devoid of an atmosphere, and thus probably also fluids in its surface layers, the principal parameter affecting the electrical conductivity will be the temperature. The maximum pressure is not sufficiently high to affect the conductivity to an appreciable degree.

The electrical conductivity of typical silicate minerals can be well approximated by:

$$\sigma = \sum_{i=1}^{2} \sigma_i \exp(-E_i/KT) \qquad 4.0.1$$

where T is the absolute temperature (measured in degrees Kelvin),

K is the Boltzman constant and the coefficients σ_i and activation energies E_i depend upon pressure and composition. The two mechanisms for electrical conduction are: intrinsic semi-conduction and ionic. Using equation 4.0.1 and appropriate values for σ_i and E_i, England et al. (1968) have derived a number of conductivity models based upon other independent temperature distributions derived from computations of the thermal history of the Moon. For this work, they used values of σ_i, E_i for olivine, an iron-magnesium silicate with

$$\sigma_1 = 5.5 \times 10^{+1} \text{ mho/meter} \qquad \text{intrinsic semi-conduction}$$
$$E_1 = 0.92 \text{ eV}$$
$$\sigma_2 = 4 \times 10^{7} \text{ mho/meter} \qquad \text{ionic} \qquad 4.0.2$$
$$E_2 = 2.7 \text{ eV}$$

And
$$\frac{\partial E_1}{\partial P} = -5.1 \times 10^{-3} \text{ ev/Kb}$$

$$\frac{\partial E_2}{\partial P} = +4.8 \times 10^{-3} \text{ ev/Kb}$$

The pressure at the center of the Moon is approximately 50 Kb so it is seen that the principal mechanism for electrical current flow is ionic in these models.

A summary of their results for the radial variation of σ, assuming a homogeneous composition moon is shown in Figure 20a for different thermal models ranging from young (0.9 Billion years, curve A) to old (4.5 Billion years) with melting. It is seen that the conductivity is very low in the outermost layers of the moon, increasing rapidly until a depth of approximately 400 Km. is reached. At greater depths the conductivity increases

much less rapidly but there are significant differences in the deep interior values depending upon the assumed age of the Moon. This is because the thermal history models used by England et al. (1968) employed radioactive heat sources with the same composition as chondritic meteorites.

The corresponding temperature profiles for the conductivity curves is shown in Figure 20b. Here the cause of the sharp increase of conductivity with depth in the near surface layers and the eventual limiting values for the core are evident. Using slightly different values of σ_i', E_i and a different lunar thermal history model, Tozer and Wilson (1967) derived a conductivity profile similar to curve C in Figure 20a. The very low thermal diffusivity of silicates essentially traps all the heat generated below approximately 400 Km. in the Moon.

The marked dependence of lunar electrical conductivity upon temperature is a relationship which can also be inverted so that given the electrical conductivity of the Moon and its composition, an estimate of its internal temperature can be made. It should be noted that for the general range of temperatures in the lunar interior, a decade change in conductivity corresponds to a 200°K change in temperature for temperatures between 1000°K-2000°K. The relationship 4.0.1 between temperature and conductivity depends upon composition such that for a suite of typical materials described geologically as being the same, they in fact yield a variation by $\pm$ one order of magnitude in σ. Thus it is clear that the variation of composition will lead to internal temperature estimates with an uncertainty of $\pm$ 200°K, even assuming that the electrical conductivity is known precisely.

In the interpretation of the early Explorer 35 measurements, Ness et al. (1967) used similar arguments to those of Gold (1966) and Tozer and Wilson (1967) regarding the diffusion time of magnetic field lines in the lunar interior to deduce the effective electrical conductivity. For the transient case, the characteristic diffusion time, τ , the "Cowling" time constant, is

$$\tau = \mu \sigma L^2 \qquad 4.0.2$$

where L is the characteristic length scale of the body assuming a one dimensional geometry. The absence of a bow shock was interpreted as indicating that the value of τ must be less than the time for transit of the field lines carried by the solar wind past the Moon. Thus

$$\tau \leq \frac{2 R_m}{V_{sw}} \qquad 4.0.3$$

which upon substitution in 3.0.2 yields

$$\sigma_{eff} \leq \frac{2}{\mu V_{sw} R_m} \qquad 4.0.4$$

assuming $L = R_m$. Using nominal solar wind parameters, this led Ness et al. (1967) to conclude that the effective lunar electrical conductivity σ must be less than 10^{-5} mhos/meter. In a more rigorous treatment of the problem of transient induction in a sphere, it is well known that the three dimensional geometry introduces a modification of the time constants so that the lowest

order mode Cowling diffusion time constant is given by:

$$\tau = \mu\sigma R^2/\pi^2 \qquad 4.0.5$$

Assuming that the scale length $L = R_M$ for a homogeneous moon, the characteristic time constants are included in Figure 20a for various values of the conductivity.

While the computed conductivity profiles show that the assumption of a homogeneous moon is not valid, they do indicate that the values for σ are many orders of magnitude higher than can be considered consistent with the observed time constant of less than 10 seconds. From this, Ness et al. (1967) concluded that the average temperature of the Moon, taking into account the three dimensional geometry, must be less than 1000°K. Colburn et al. (1967) supported the conclusion of a low bulk electrical conductivity for a homogeneous moon. However, they considered attempts to determine an interior temperature based on this effective conductivity premature, because the inhomogeneous Moon might produce no bow shock but still possess a highly conductive lunar interior. The next section discusses this possibility in detail.

4.1 Unipolar Inductor: Steady State

As the solar wind convectively transports the imbedded, frozen-in interplanetary magnetic field past the Moon, it generates an electric field in a coordinate system fixed to the Moon. At 1 A.U., the magnitude of this field:

$$\vec{E} = -\vec{V}_{sw} \times \vec{B}_o \qquad 4.1.1$$

is 1 millivolt/meter for typical solar wind parameters. This electric field, unless opposed by a polarization of the Moon as a dielectric, will lead to electrical currents which generate a secondary magnetic field. This induced current system and the effect it would have on the solar wind flow was first considered quantitatively by Sonett and Colburn (1967) for a homogeneous Moon and by Hollweg (1968) and Sonett and Colburn (1968) for an inhomogeneous Moon.

The reality of the unipolar mechanism depends upon the ability of the electrical current to form a closed circuit by means of a return path in the solar plasma. Although the exact nature of the plasma-moon interface is not yet known, it has been assumed that the equivalent electrical impedance is much less than that associated with the current flow in the lunar interior. It is of course well known that the conductivity of the solar plasma is very high. Indeed it is this characteristic of the solar plasma which leads to the "frozen-in" magnetic field and the unipolar induction mechanism itself.

The quantitative study by Hollweg (1968) assumed the Moon to be a simple, two concentric layered cylinder, representing the core and crust. Using as the inducing field equation 4.1.1, he derived extreme values of the conductivity of the core and crust, for limiting cases of the ratio of crustal to core conductivity. The extreme value was based upon the absence of plasma flow deflection, according to equation 2.1.1, as the necessary condition determining the presence or absence of a bow or limb shock. His results for the steady-state flow may

be summarized as follows:

1. For a conducting thin crust, supporting the major fraction of current flow, the interior conductivity must be much less than 10^{-5} mhos/meter.
2. For a low but finite conductivity crust, with the core supporting the major fraction of current flow, the core conductivity must be much less than 2.6×10^{-5} mhos/meter.
3. For a thin insulating crust, shielding a conductive core, the crust conductivity must be less than 10^{-10} mhos/meter for a 10 meter thick crust and 10^{-7} mhos/meter for a 10 Km. thick crust.

Since such low conductivities as required by case 3 seemed unlikely, Hollweg (1968) concluded that the presence of a conducting core (i.e. $\sigma_c > 10^{-5}$ mhos/meter) was highly unlikely.

For non-steady flow, Hollweg (1968, 1970) introduced the concept of "conducting islands", which were suggested to be localized disk-like near-surface regions of relatively high conductivity, 10^{-3} - 10^{-4} mhos/meter. They would, by the unipolar mechanism, generate an induced field sufficient to deflect the solar wind flow at the limbs of the Moon and thus explain the observed penumbral increases in the interplanetary magnetic field discussed in section 3.1. These "conducting islands" thus represent a physical basis for the suggestion by Siscoe et al. (1969) of an ad hoc mechanism for solar wind flow deflection at the lunar limbs. Hollweg noted that limb shocks thus generated would form only in the vicinity of the plane defined by $\vec{V}_{sw}$ and $\vec{B}_0$, the plane of symmetry.

Schwartz et al. (1969) have repeated the earlier study by Sonett and Colburn (1968) on the unipolar induction mechanism, expanding it to include several different thermal profiles and conductivity functions. They conclude that a moon possessing a hot interior, but with a cool exterior, can cause the reported plasma deflection at the lunar limb by the unipolar mechanism. This will generate the observed limb shock wave, which is their description of the phenomena of penumbral increases. While they do not give the conductivity profile for their preferred model, based upon a diabase composition, the relationship of conductivity to temperature for this material and conductivity model is given.

$$\sigma_D = 10^3 \exp(-0.634/KT) \qquad 4.1.2$$

The internal temperatures in all their models employed is approximately 1700°-1900° K for depths greater than 400 Km. so it is clear that Schwartz et al. (1969) predict a hot lunar interior with an electrical conductivity of $\sim$10 mhos/meter.

The results of Whang and Ness (1970) on the lunar Mach cone geometry are especially significant in the framework of interpretations of the magnetic field penumbral increases and the possibility of the lunar unipolar induction mechanism. The induced magnetic field due to the unipolar mechanism is toroidal with the axis of symmetry perpendicular to the plane of symmetry defined by $\vec{V}_{sw}$ and $\vec{B}_o$. The magnitude of the field, using the symbols defined in Figure 16, is proportional to the magnetic field, solar wind velocity and angle θ as:

$$H_\phi \propto \vec{B}_o \times \vec{V}_{sw} \cos\theta \qquad 4.1.3$$

so that the magnetic back pressure for plasma deflection is

$$P_{MAG} \propto V_{sw}^2 \quad B^2_{\circ} \sin^2 \phi_{\circ} \cos^2 \theta \qquad 4.1.4$$

The solar wind pressure normal to the lunar surface (and the toroidal magnetic field) depends upon the angle Δ of the normal measured with respect to the limb of the Moon as:

$$P_{sw} \propto n V_{sw}^2 \sin^2 \Delta \qquad 4.1.5$$

Thus for deflection to take place we equate 4.1.4 and 4.1.5 to obtain:

$$\sin \Delta \propto \frac{B_{\circ}}{\sqrt{n}} \sin \phi_{\circ} \cos \theta \qquad 4.1.6$$

relating the deviation of the flow and the properties of the magnetized solar wind and the position of the observation point relative to the plane of symmetry.

However, $\sin \phi_{\circ} \cos \theta = \cos \psi$, the angle of propagation used by Whang and Ness (1970) in their Mach cone geometry study (See Section 3.4). Thus for small angles of deflection, where $\sin \Delta = \Delta$, one finally obtains:

$$\Delta \propto \frac{B_{\circ}}{\sqrt{n}} \cos \psi \qquad 4.1.7$$

The Mach cone, as defined and analyzed by Whang and Ness (1970) is the surface separating penumbral increases and decreases

in the lunar wake. It is reasonable to assume that this surface would be the same or linearly related to the surface defined by the deflected plasma. In this case Δ is a maximum at $\psi = 0°$ and a minimum at $\psi = 90°$.

It will be recalled from Figure 19 that the observed variation of the Mach cone angle α with ψ is elliptical with a maximum at $\psi = 90°$ and a minimum at $\psi = 0°$. This is exactly the opposite relationship from that to be expected if unipolar induction is an important mechanism affecting the solar wind interaction with the Moon and responsible for the penumbral increases. Examples of clearly observable penumbral anomalies for the case of aligned field and flow are shown in Figure 21. Under the assumption that the unipolar induction mechanism is responsible for penumbral increases, they should not be observed for $\phi_o = 0°$ (or 180°). Their existence provides further evidence that some other mechanism must be responsible for the observed penumbral increases than plasma deflection due to induced magnetic fields. In Whang's 1969 model, he proposed an ad-hoc field perturbation of the limb which propagated back along the Mach cone surface. This appears to be an attractive suggestion since any deflection of plasma would also lead to an enlarged Mach cone inconsistent with the velocity of propagation of disturbances in the solar wind.

A possible source, which has yet to be considered, is the effect of the finite Larmor Radius of the solar wind ions and the almost unique coincidence of their cyclotron period with the convection time past the Moon. Clearly for such a small scale

effect as the penumbral increases imply in the overall solar wind interaction problem, this feature of the flow must be considered in future studies.

4.2 Time Varying Induction

An alternative method to investigate the electrical conductivity of the lunar interior, from that of studying the steady state characteristics of the solar wind interaction discussed in Sections 4.0 and 4.1, is to employ the naturally occurring fluctuations of the interplanetary magnetic field. In studies of deep terrestrial mantle conductivity, large quasi-sinusoidal variations with periods of days and weeks are driven by ionospheric current systems. These primary currents induce secondary currents in the earth by Faraday's Law whose associated magnetic field is used to deduce the nature of the subsurface electrical conductivity. Naturally occurring electromagnetic signals at much higher frequencies generated by lightning have been used to study the shallow mantle conductivity.

In the case of the Moon, the interplanetary medium moves supersonically past the body so that all explicit time variations observed in a coordinate system fixed to the Moon are directly related to the spatial variation of the interplanetary medium rather than its temporal variations. There exists little evidence for the existence of waves with quasi sinusoidal variations in the solar wind. Rather the interplanetary medium appears to be micro-structured into a large number of regions of magnetized-plasma, separated from each other by classical MHD discontinuities, which are convectively transported outward from the sun. The discontinuities are most clearly observed

as very sudden changes in the interplanetary magnetic field (and plasma) which occur in less than 10-100 seconds. In order to use such discontinuities, it is necessary that the three following conditions be satisfied:

1. Explorer 35 be located within the plasma umbra or penumbra so that secondary fields can be measured,
2. An independent simultaneous observation in cis-lunar space be made of the time profile of the discontinuity to establish a reference scale for the changes, and
3. A discontinuity with a short time constant, $\lesssim$ 10 seconds, is convected past the moon at a time such that it can be observed by Explorer 35.

Ness (1968, 1969) has used these discontinuities to obtain an independent estimate of the conductivity of the lunar interior.

Simultaneous data from Explorers 33 and 35 which satisfy the above criteria is shown in Figure 22. The 2 events were selected from a total of 6 which were the only ones observed during the period July 1967-June 1968. In both cases the field change associated with the discontinuity surface is observed principally as a change in the latitude, θ_{SE}, of the field vector. Each event shows that both satellites observe the discontinuities to be identical using 81.8 second averages of the measured magnetic field. Superposed are the steady state perturbations of the magnetic field in the lunar wake consisting of the indicated umbral and penumbral anomalies. It should also be noted that during the several hours of interplanetary magnetic field data, the two satellites measure essentially the same magnetic field, except for the time offsets noted

at the top. This is a characteristic feature of the interplanetary medium, that it is uniform on the scale of cis-lunar distances except for the imbedded planar discontinuity surfaces.

A more detailed time profile of these two events is presented in Figure 23 from the fine time resolution data obtained at 5.11 second intervals. This shows that for the February event there is a measurable time dilation of the discontinuity from less than 10.2 to 56.2 seconds observable in both the X and Z components. For the event in May the time profile is identical within the resolution of the data: 40.9 and 36.8 seconds.

The first event is interpreted in terms of the lowest order mode Cowling diffusion time constant being less than 1/3 of the 56.2 second time interval during which the eddy currents induced in the Moon and their magnetic fields decay to zero. This value of $\tau_D < 20$ seconds compares very favorably with that determined independently from the steady state flow (See Section 4.0). Assuming a two layer moon with negligible crust conductivity and a core radius of approximately 1350 Km. yields an interior conductivity of 8×10^{-5} mhos/meter. This corresponds to a temperature estimate of $800° \pm 200°$ K using typical values for olivine. These results were first reported by Ness (1969).

The second event in May 1968 shows no similar time dilation effect. This is believed due primarily to the long time width of the discontinuity (>10 sec) as well as to the distance of the satellite from the umbra. At the time of observation it was located 0.7 R_M from the cavity axis while for the February 1968 event; it was only 0.3 R_M from the cavity axis. The induced

fields of the Moon are small at satellite altitude and confined to the interior of the plasma cavity. When Explorer 35 is located either in the penumbra or far downstream from the Moon, there is no measurable effect on discontinuity time profiles which can be associated with the lunar interior (Ness, 1968). There is as yet no theory for the transient response of the Moon to discontinuities in the interplanetary medium.

Studies of the induced fields in the Moon due to sinusoidal variations of the external magnetic (and/or electric) field have been considered by several authors with certain simplifying assumptions. Blank and Sill (1969a) studied the secondary magnetic fields induced in a homogeneous moon by a sinusoidally varying magnetic field with the assumption that the secondary magnetic fields were axially symmetric and confined to meridian planes. They failed to include the motional electric field induced by the flow of the solar wind past the Moon and also used the wrong boundary conditions. The appropriateness of their analysis was questioned by Fuller and Ward (1969); and replied to by Blank and Sill (1969b). Subsequently Sill and Blank (1970) presented a revised analysis of the problem taking these criticisms into account and also adding the refinement of a radially inhomogeneous Moon.

In a similar and slightly earlier sequence of studies, Schwartz and Schubert (1969) and Schubert and Schwartz (1969) studied the secondary fields induced in the Moon by a sinusoidal varying electric and magnetic field for a homogeneous and a

radially inhomogeneous moon. Although they used the correct inducing fields (both $\vec{B}$ and $\vec{E}$) in their studies, their boundary condition also imposed a non-realistic constraint since it did not correctly reflect the strong asymmetry due to the supersonic plasma impact on the sun-light surface of the Moon while the secondary fields expand into a vacuum on the night side. They showed that the fluctuations of the magnetic field generated a secondary poloidal (dipole) field while the electric field fluctuations generated a secondary toroidal magnetic field.

In addition, these studies by Blank-Sill and Schwartz-Schubert all require:

1. The wavelength of the inducing field must be much larger than the radius of the Moon so that a uniform field penetrates the interior of the Moon and
2. The time scale of the field variations must be much larger than the Cowling diffusion time, i.e. a low frequency limit where $f \ll 0.01$ seconds.

While no experimental results are thus far available to compare with these theories, even in their rudimentary form, it may be expected that future measurements on the lunar surface in the Apollo program may provide data relevant to these studies when compared to simultaneous measurements in orbit from Explorer 35. However, until the boundary value problem is correctly formulated, such data will not be capable of being uniquely interpreted.

It should be noted that these theories assume a priori that the magnetic fluctuations (and their associated electric fields) uniformly excite the lunar interior. However, it is

by no means clear that this requirement is met for the Moon since as the plasma is absorbed at the sunlight lunar surface, the fluctuations are converted to electromagnetic waves. However, on the dark side of the moon, there is no corresponding excitation so that there is hemispherical asymmetry of the source. On the sunlight side, the normal component of the secondary magnetic field must be zero since the conductivity of the solar plasma is very high. On the night side, however, only the divergence free constraint on $\vec{B}$, namely $\vec{B}_I \cdot \vec{n} = \vec{B}_E \cdot \vec{n}$ is required where $\vec{B}_E$ is the external field and $\vec{B}_I$ the internal field, and $\vec{n}$ is the normal to the lunar surface. Thus a strong asymmetry exists also in the boundary conditions.

The net inducing field is thus rather substantially modified from that assumed by Blank, Sill, Schwartz and Schubert. Although the problem of the EM response of a conducting sphere in a time varying electromagnetic field in an old classic problem (for example, see Debye (1908) and Wait (1951)) the case of the Moon is sufficiently different that the simple modifications thus far studied are probably not approppriate to represent the real problem.

5.0 Summary

Early satellite studies related to the solar wind interaction with the Moon before 1967 did not correctly reveal the characteristic features of the phenomenon. The USA Lunar Explorer 35 has provided since July 1967 definitive experimental results regarding the perturbations of the interplanetary magnetic field and plasma in the lunar wake. The Moon appears to behave as a non-magnetic, non-electrically conducting fully absorbing spherical obstacle in the solar wind flow. The principal features of the plasma-field perturbations are: (See Figure 24):

1. A downwind plasma umbral cavity or void containing an enhanced interplanetary magnetic field ($<+30$ %) only slightly perturbed in direction, (no bow shock wave, pseudo-magnetosphere or trailing shock is observed),
2. A downwind penumbral region aft of a rarefaction wave or Mach cone, elliptical in cross-sectional geometry, contains a reduced plasma flux and magnetic field (>-30 %),
3. A very limited penumbral region, upwind of the lunar Mach cone, sometimes contains an enhanced ($<+30$ %) magnetic field and plasma flux and
4. A broad region both upstream and downstream from the lunar wake but connected to it by the interplanetary magnetic field in which rapid fluctuations ($\frac{\Delta|B|}{B_o} \sim 0.2$) of the magnetic field occur with an amplitude that decreases with distance from the wake.

It is found that:

5. The Moon hardly effects the time profile of discontinuity surfaces as they are convectively transported past the Moon (or a shock wave as it propagates past the Moon), and
6. The <u>axis of the plasma cavity</u>, as measured by the lunar Mach cone is aberrated by 4.5° ± 0.5° from the Moon-Sun line.

The magnitude of the anomaly (1) is linearly dependent upon the plasma diamagnetic properties as measured by:

$$\left.\frac{\Delta|B|}{B_o}\right|_{umbra} \doteq (0.23 \pm 0.09)\, \beta_{i+e} \qquad 5.0.1$$

From this relationship, in comparison with theory, it has been possible to derive the temperature of the solar wind electrons with the result that $T_e \doteq 2\, T_i$.

The observations and interpretations of the lunar Mach cone elliptical geometry present, for the first time, experimental evidence for the anisotropic propagation of waves in the magnetized collisionless solar plasma. Parallel to the field the velocity is found to be 41 Km/sec. The anisotropy of 1.4 is consistent with that expected from the average β (~ 1) of the solar wind and the average thermal anisotropy of the warm magnetized plasma ($T_{//}/T_{\perp} \sim 1.2$). ($V_{\perp}$ = 60 Km/sec.)

The absence of a bow shock and the transit of discontinuities past the Moon with almost negligible effect by the Moon suggest a low internal electrical conductivity of less

than 10^{-4} mhos/meter and an internal temperature less than 800° ± 200° K. Unipolar induction is not a significant mechanism affecting the solar wind interaction.

This low temperature indicates either that the Moon was formed only recently, if its radioactive composition is similar to chondritic meteorites, or that if it is old, as recent age dating of its surface materials indicates, then its radioactive composition is much less than that of chondritic meteorites. Urey and MacDonald (1970) have recently reviewed all the relevant data concerning the present physical state of the Moon. They discuss the evidence that there is general agreement on the maximum temperature obtained from both the stress differences within the Moon and the electrical conductivity. They conclude that the Moon's interior is relatively cold and that there is no extensive region where the temperature exceeds 1000- 1200°C.

5.1 Future Problems

The data obtained from Explorer 35 and its interpretations have clarified most features of the solar wind interaction with the Moon. However, certain problems remain to be solved, some of which are associated with Explorer 35 having a peri-selene greater than 700 Km. These problems are:

1. What is the source mechanism producing the positive penumbral anomalies sometimes observed in the interplanetary magnetic field? (See Sections 3.1 and 4.1)
2. What is the nature of the source of the stimulated waves propagated away from the lunar wake? (See Section3.3)

3. What is the nature of the solar wind-lunar surface boundary? Are finite Larmor radii effects responsible for the penumbral increases?
4. How far behind the Moon is its wake detectable and by what means? Does a trailing shock ever exist? (See Section 3.2)
5. Is Io another Moon-like object in its interaction with the Jovian magnetosphere? (Schatten and Ness, 1970) Or Mercury with the Solar Wind?
6. What is the detailed internal electrical conductivity profile? (See Section 4.0)
7. What is the nature of the detailed plasma flow in the lunar wake region and how are the plasma parameters related to other observed phenomena in the magnetic field?

6.0 Acknowledgements

I appreciate the hospitality of the staff of the CNR-University of Rome-Laboratory for Space Plasmas in the preparation of this manuscript and the discussions of the Mach cone phenomena with Dr. Y.C. Whang.

7.0 References

Behannon, K.W., Intrinsic Magnetic Properties of the Lunar Body, J. Geophys. Res. 73, 7257, 1968.

Blank, J.L. and W.R. Sill, Response of the Moon to the time varying interplanetary magnetic field, J. Geophys. Res., 74, 736, 1969a.

Blank, J.L. and W.R. Sill, Reply, J. Geophys. Res., 74, 5175, 1969b.

Colburn, D.S., R.G. Currie, J.D. Mihalov and C.P. Sonett, Diamagnetic Solar Wind Cavity Discovered behind Moon, Science, 158, 1040, 1967.

Debye, P., Der Lichtdruck auf Kugeln von beliebigen Material Ann. d. Phys. 30, 57, 1909.

Dessler, A.J., Ionizing plasma flux in the Martian upper atmosphere, in Atmos. of Venus and Mars ed. by J.C. Brandt and M.B. McElroy, p. 241, Gordon and Breach, London 1967.

Dolginov, Sh.Sh., Ye. G. Yeroshenko, L.N. Zhuzgov and N.V. Pushkov, Investigation of the Magnetic Field of the Moon, Geomagnetism i Aeronomiya, 1, 21, 1961.

Dolginov, Sh.Sh., Ye. G. Yeroshenko, L.N. Zhuzgov and L.O. Tyurmina, Magnetic Measurements with the Second Cosmic Rocket, Iskusstvennye Sputniki Zemli, 5, 16 (Artificial Earth Satellites, p. 490, 1960), 1960.

Dolginov, Sh.Sh., Ye. G. Yeroshenko, L.N. Zhuzgov and I.A. Zhulin, Possible Interpretation of the Results of Measurements on the Lunar Orbiter Luna 10, Geomagnetism and Aeronomy, 7, 436, 1967.

England, A.W., G. Simmons and D. Strangway, Electrical Conductivity of the Moon, J. Geophys. Res., 73, 3219, 1968.

Fahleson, U., Laboratory Experiments with plasma flow past unmagnetized obstacles, Planet. Space Sci., 15, 1489, 1967.

Fuller, B.D. and S.H. Ward, Discussion of Paper by J.L. Blank and W.R. Sill, Response of the Moon to the time varying Interplanetary Magnetic Field, J. Geophys. Res., 74, 5173, 1969.

Gringauz, K.I., V.V. Bezrukikh, M.Z. Khokhlov, G.N. Zastenkev, A.P. Remizov and L.S. Muzatov, Experimental Results concerning the lunar ionosphere detected on the first artificial lunar satellite, Dokl. Akad. Nauk. SSSR, 170, 1306, 1966.

Gold, T., The Magnetosphere of the Moon in The Solar Wind ed. by R.I. Mackin, Jr. and M. Neugebauer, Pergamon Press, N.Y. p. 381, 1966.

Greenstadt, E.W., Interplanetary Magnetic Effects of Solar Flares: Explorer 18 and Pioneer 5, J. Geophys. Res., 70, 5451, 1965.

Hirshberg, J., Discussion of paper by N.F. Ness "The magneto-hydro dynamic wake of the Moon", J. Geophys. Res., 71, 4202, 1966.

Hollweg, J. V., Interaction of the solar wind with the moon and formation of a lunar limb shock wave, J.Geophys. Res., 73, 7269, 1968.

Hollweg, J.V., Lunar Conducting Islands and the formation of a lunar limb shock wave, J. Geophys. Res., 75, 1209,1970.

Ivanov, K.G., Did the IMP-1 observe the Magnetic Wake of the Moon or Earth?, Geomagnetism and Aeronomy, 5, 581, 1965.

Johnson, F., and J.E. Midgley , Notes on the Lunar Magneto-sphere J. Geophys. Res., 73, 1523, 1968.

Krall, N.A. and Derek A. Tidman, Magnetic Fluctuations near the Moon, J. Geophys. Res., 74, 6439, 1969.

Lin, R.P., Observations of lunar shadowing of energetic particles, J. Geophys. Res., 73,3066, 1968.

Lüst, V.R., Über die Ausbreitung von Wellen in einem Plasma, Furtschritte der Physik, 7, 503, 1959.

Lyon, E.F., H.S. Bridge and J.H. Binsack, Explorer 35 Plasma Measurements in the Vicinity of the Moon, J. Geophys. Res., 72, 6113, 1967.

Michel, F.C., Interaction between the solar wind and the lunar atmosphere, Plan. Space Sci., 12, 1075, 1964.

Michel, F.C., Detectability of disturbances in the Solar Wind, J. Geophys. Res., 70, 1, 1965.

Michel, F.C., Shock wave trailing the Moon, J. Geophys. Res., 72, 5508, 1967.

Michel, F.C., Magnetic Field Structure behind the Moon, J. Geophys. Res., 73, 1533-1542, 1968a.

Michel, F.C., Lunar Wake at large distances, J. Geophys. Res., 73, 7277, 1968b.

Ness, N.F., The Magnetohydrodynamic Wake of the Moon, J.Geophys.Res, 70, 517, 1965a.

Ness, N.F., Remarks on preceding paper by E.W. Greenstadt, J. Geophys. Res., 70, 5453, 1965b.

Ness, N.F., Reply, J. Geophys. Res., 71, 4205, 1966a.

Ness, N.F., Remarks on paper by K.G. Ivanov, Geomagnetism and Aeronomy, 6, 301, 1966b.

Ness, N.F., Remarks on the Interpretation of the Luna 10, Geomagnetism and Aeronomy, 7, 452, 1967.

Ness, N.F., Recent Results from Lunar Explorer 35, NASA-GSFC preprint X616-68-335. To be published in Proceedings of Kiev Conference on the Moon and Planets, October, 1968.

Ness, N.F., Lunar Explorer 35, Space Research, 9, 678-703, 1969.

Ness, N.F.,K.W. Behannon, C.S. Scearce and S.C. Cantarano, Early results from the Magnetic Field Experiment on Explorer 35, J. Geophys. Res., 72, 5769, 1967.

Ness, N.F.,K.W. Behannon, H.E. Taylor and Y.C. Whang, Perturbations of the Interplanetary Magnetic Field by the Lunar Wake, J. Geophys. Res., 73, 3421, 1968.

Ness, N.F., C.S.Scearce and J.B. Seek, Initial results of the IMP-1 Magnetic Field Experiment, J. Geophys. Res., 69, 3531, 1964.

Ness, N.F. and K.W. Schatten, Detection of Interplanetary Magnetic Field Fluctuations Stimulated by the Lunar Wake, J. Geophys. Res., 74, 6425, 1969.

Neugebauer, M., Question of the Existence of a Lunar Magnetic Field, Phys. Rev. Left., 4, 6, 1960.

Ogilvie, K.W. and N.F. Ness, Dependence of the lunar wake on Solar Wind Plasma Characteristics, J. Geophys. Res., 74, 4123,1969.

Schatten, K.W. and N.F. Ness, Modulation of Jupiter's Radio Emission by Io, Trans. AGU, 52, 481,1970.

Schneider, O., Interaction of the Moon with the Earth's Magnetosphere, Space Sci. Revs., 6, 655, 1967.

Schubert, G. and K. Schwartz, A theory for the interpretation of lunar surface magnetometer data, The Moon, 1, 106, 1969.

Schwartz, K. and G. Schubert, Time-dependent lunar electric and magnetic fields induced by a spatially varying interplanetary magnetic field, J. Geophys. Res., 74, 4777, 1969.

Schwartz, K., C.P. Sonett and D.S. Colburn, Unipolar Induction in the Moon and a lunar limb shock mechanism, The Moon, 1, 7, 1969.

Sill, W.R. and J.L. Blank, Method for estimating the electrical conductivity of the lunar interior, J. Geophys. Res., 75, 201, 1970.

Siscoe, G.L., E.F. Lyon, J.H. Binsack and H.S. Bridge, Experimental evidence for a detached lunar compression wave, J. Geophys. Res., 74, 59, 1969.

Sonett, C.P. and D.S. Colburn, Establishment of a lunar Unipolar Generator and Associated Shock and Wake by the Solar Wind, Nature, 216, 340, 1967.

Sonett, C.P. and D.S.Colburn, The Principle of Solar Wind Induced Planetary Dynamos, Phys. Earth Planet. Interiors, 1, 326, 1968.

Sonett, C.P., D.S. Colburn and R.G. Currie, The Intrinsic Magnetic Field of the Moon, J. Geophys. Res., 72, 5503, 1967.

Spreiter, J. and A. Alksne, Plasma flow around the magnetosphere, Revs. Geophys., 7, 11, 1969.

Taylor, H.E., Aspect determination in lunar shadow on Explorer 35, NASA-TN D-4544, 1968.

Taylor, H.E., K.W. Behannon and N.F. Ness, Measurements of the perturbed Interplanetary Magnetic Field in the Lunar Wake, J. Geophys. Res., 73, 6723, 1968.

Tozer, D.C. and J. Wilson, III. The Electrical Conductivity of the Moon, The Electrical Conductivity of the Moon's Interior, Proc. Roy. Soc. (London) Ser. A, 296, 320, 1967.

Urey, H.C. and G.J.F. MacDonald, Origin and history of the Moon, revised chapter 13 in Physics and Chemistry of the Moon, ed. by Z. Kopal, Academic Press (1970).

Van Allen, J.A. and N.F. Ness, Particle Shadowing by the Moon, J. Geophys. Res., 74, 71, 1969.

Wait, J.R., A Conducting Sphere in a time varying field, Geophysics, 16, 4, 666, 1951.

Whang, Y.C., Interaction of the Magnetized Solar Wind with the Moon, Phys. Fluids, 11, 969, 1968a.

Whang, Y.C., Theoretic 1 Study of the magnetic field in the Lunar Wake, Phys. Fluids, 11, 1713, 1968b.

Whang, Y.C., Field and Plasma in the lunar wake, Phys. Rev., 186, 143, 1969.

Whang, Y. C., and N. F. Ness, Observations and Interpretations of the Lunar Mach Cone, NASA-GSFC preprint X-692-70-60, 1970.

Zhuzgov, L. N., Sh. Sh. Dolginov and Ye. G. Yeroshenko, Investigation of the Magnetic Field from the Satellite Luna 10, Kosmicheskiye Issledovaniya, 4, 880, 1966.

8.0 List of Figures

10. - Theoretical magnetic field profiles in lunar wake computed in plane of symmetry from first order approximation to perturbed plasma ion wake (Whang, 1968b; 1969). The dashed curves in the lower figure represent the direction of plasma flow velocity.

11. - Diagram developing further geometry and flow characteristics behind the Moon leading to formation of a trailing shock wave (Wolf, 1968). The upper figure refers to the plane of symmetry while the lower figure refers to a plane perpendicular to this.

12. - Simultaneous magnetic field (NASA-GSFC) and plasma data (MIT) showing correlated penumbral increases (Siscoe et al., 1969).

13. - Geometry for computation of impact parameter of field line threading the Moon (a) and experimental results from Explorer 35 (b) (Van Allen and Ness, 1969).

14. - Illustration of method using simultaneous magnetic field and low-rigidity solar electron flux observations on Explorer 35 to distiguish between models for interplanetary field line geometry near Moon (Van Allen and Ness, 1969).

15. - Stimulated waves observed in the fluctuations of the magnitude of the interplanetary magnetic field both upstream (pre-shadow) and downstream (post-shadow) from the lunar wake (Schatten and Ness, 1969).

16. - Example of identication of lunar Mach cone crossing observed in magnetic field signatures in lunar wake (Whang and Ness, 1970).

17. - Geometry for analysis of variation of lunar Mach cone angle, α, relative to spacecraft position, sc, field line orientation and plane of symmetry. The propagation angle, ψ, is defined as shown.

18. - Summary of Mach cone crossings corresponding to propagation angle, ψ, of approximately 90° (Whang and Ness, 1970).

19. - Variation of relative Mach angle (α / α^*, where $\alpha^* = 8°$) as function of angle of propagation, ψ, defined in figure 17. The elliptical variation of (α / α^*) with ψ is

evidence of the anisotropic propagation velocity of magnetoacoustic waves in the solar wind (Whang and Ness, 1970).

20. - Electrical conductivity profile of Moon as function of depth (a) for various model cases using typical mantle-like parameters for iron-magnesium silicates and thermal history based on chondritic meteorite radioactivity composition (England et al., 1968). The corresponding temperature profiles are shown in (b).

21. - Observation of identifiable penumbral increases in the interplanetary magnetic field as observed by the NASA-GSFC magnetic field experiment when the field direction is almost aligned with solar wind velocity.

22. - Simultaneous Explorers 33 and 35 measurements of interplanetary magnetic field as discontinuity passes Moon at moment the latter spacecraft is located within lunar wake region (Ness, 1969).

23. - Detailed magnetic field data on an expanded time scale (by factor of 16 from that used in Figure 22) showing effect of lunar body in distorting time profile when spacecraft is in core of wake (a) and lack of effect when spacecraft is in penumbra (b) (Ness, 1969).

24. - Summary view of solar wind " weak" interaction with the Moon. As the lunar surface absorbs all plasma (and particle) flux which strike it, a plasma cavity develops and small (< 30 %) magnetic field perturbations are observed in the plasma umbra and penumbra (characteristically +-+-+).

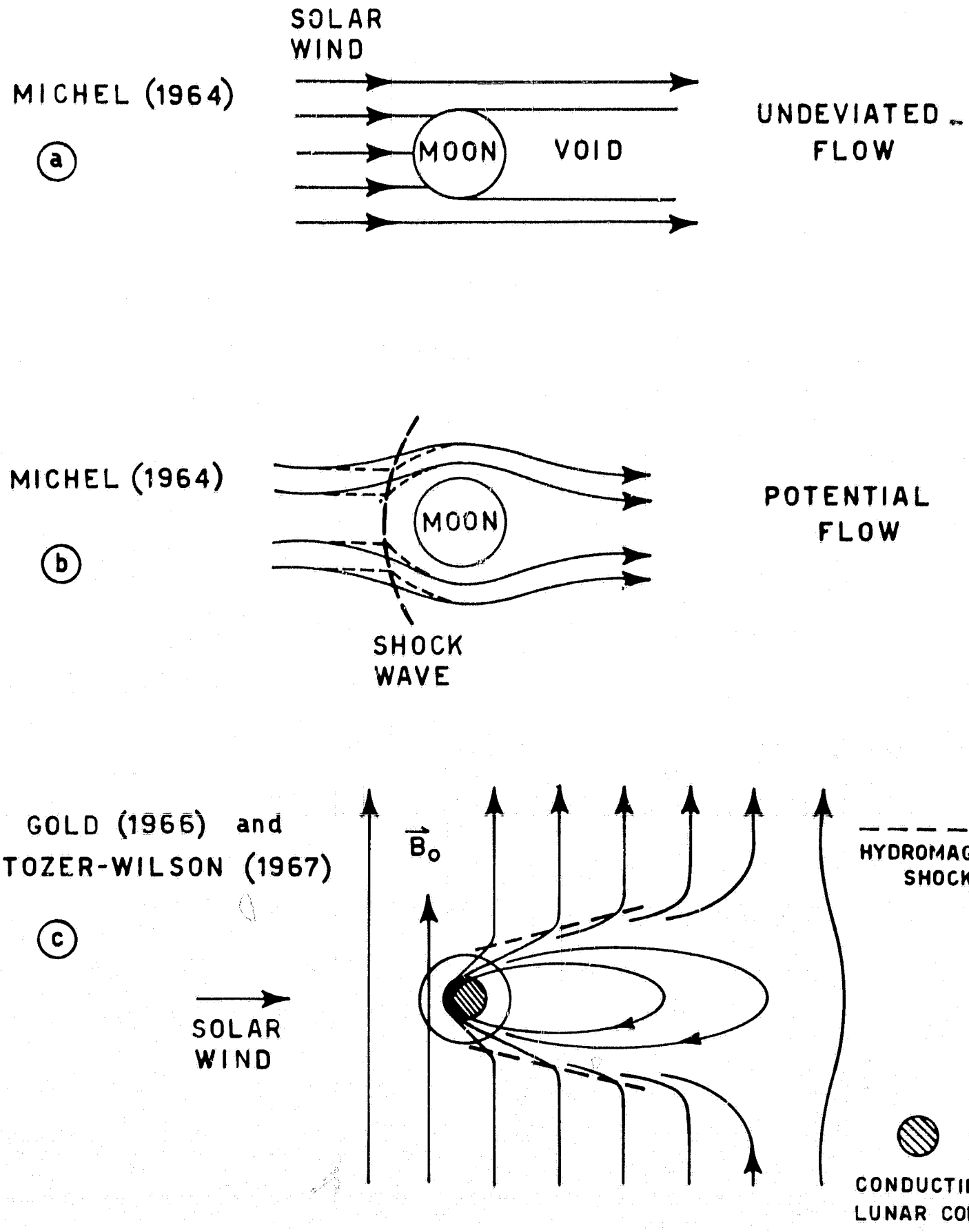
MICHEL (1964)
(a)
SOLAR WIND
MOON
VOID
UNDEVIATED FLOW
MICHEL (1964)
(b)
MOON
POTENTIAL FLOW
SHOCK WAVE
GOLD (1966) and
TOZER-WILSON (1967)
(c)
$\vec{B}_o$
HYDROMAGNETIC SHOCK
SOLAR WIND
CONDUCTING LUNAR CORE

FIGURE 1

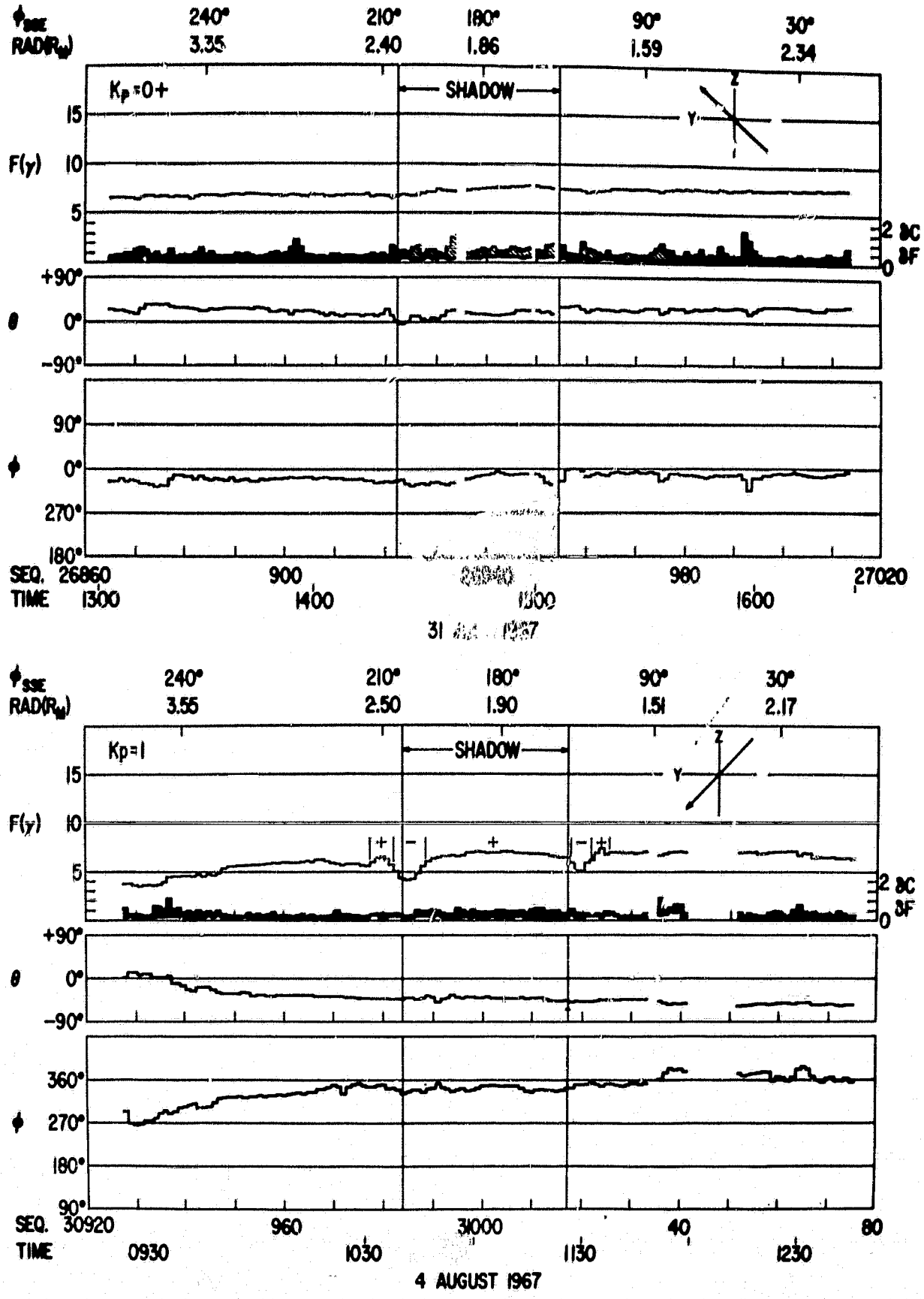
ϕ_{SSE}
RAD(R_M)
240°
3.35
210°
2.40
180°
1.86
90°
1.59
30°
2.34
K_p=0+
SHADOW
Z
Y
F(y)
15
10
5
2 δC
0 δF
θ
+90°
0°
-90°
φ
90°
0°
270°
180°
SEQ. 26860
900
980
27020
TIME 1300
1400
1500
1600
31 AUG 1967
ϕ_{SSE}
RAD(R_M)
240°
3.55
210°
2.50
180°
1.90
90°
1.51
30°
2.17
Kp=1
SHADOW
Z
Y
F(y)
15
10
5
2 δC
0 δF
θ
+90°
0°
-90°
φ
360°
270°
180°
90°
SEQ. 30920
960
31000
40
80
TIME 0930
1030
1130
1230
4 AUGUST 1967

FIGURE 2

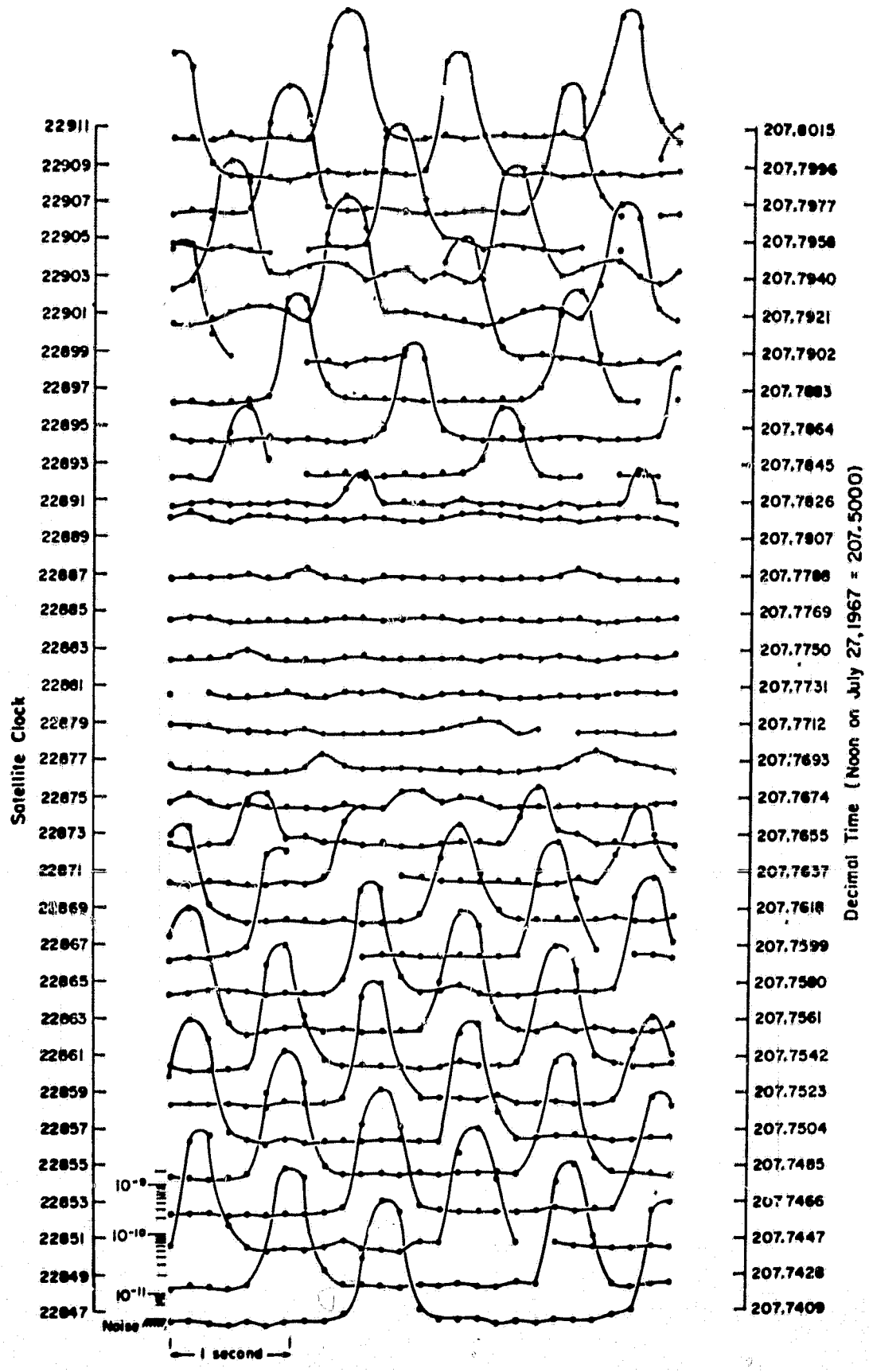
Satellite Clock
22911
22909
22907
22905
22903
22901
22899
22897
22895
22893
22891
22889
22887
22885
22883
22881
22879
22877
22875
22873
22871
22869
22867
22865
22863
22861
22859
22857
22855
22853
22851
22849
22847
10^{-9}
10^{-10}
10^{-11}
Noise
1 second
207.8015
207.7996
207.7977
207.7958
207.7940
207.7921
207.7902
207.7883
207.7864
207.7845
207.7826
207.7807
207.7788
207.7769
207.7750
207.7731
207.7712
207.7693
207.7674
207.7655
207.7637
207.7618
207.7599
207.7580
207.7561
207.7542
207.7523
207.7504
207.7485
207.7466
207.7447
207.7428
207.7409
Decimal Time (Noon on July 27, 1967 = 207.5000)

FIGURE 3

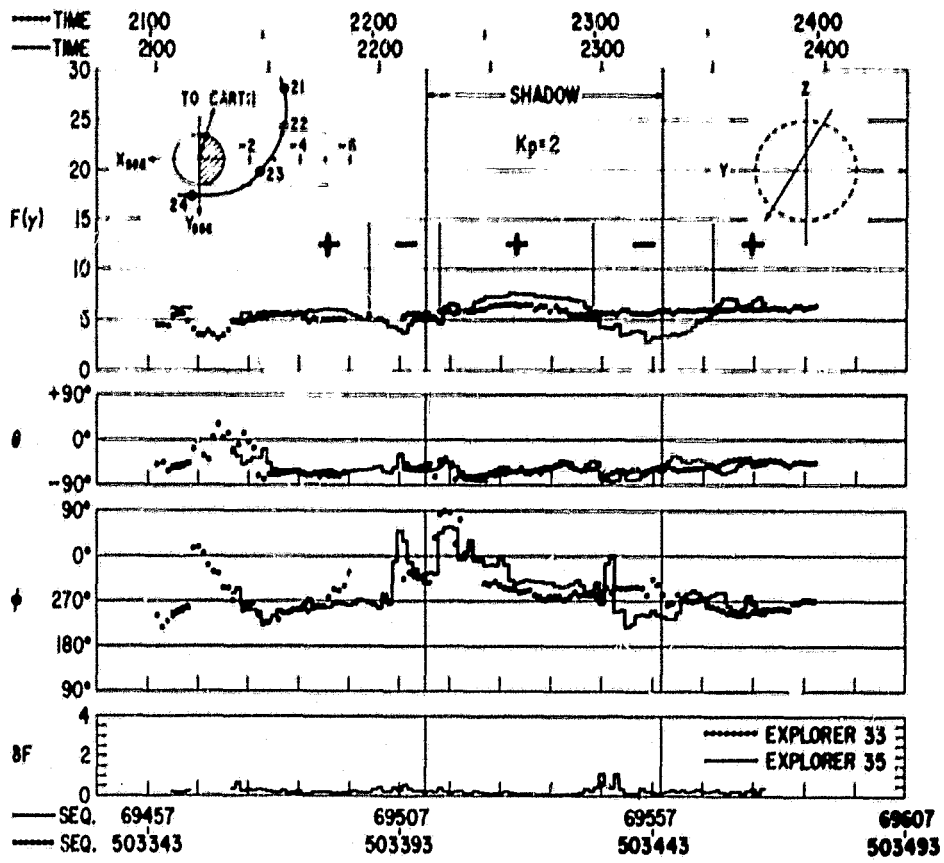

EXPLORERS 33 & 35 - 9 SEPTEMBER 1967

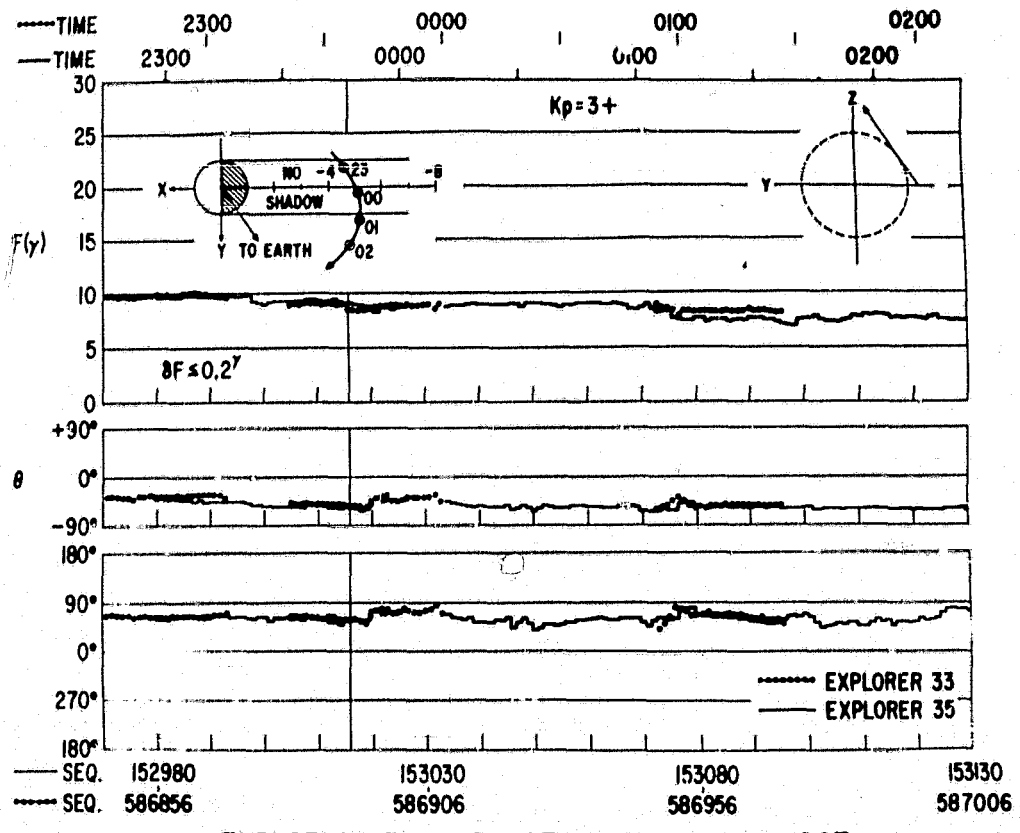

EXPLORERS 33 & 35 - 27,28 NOVEMBER 1967

FIGURE 4

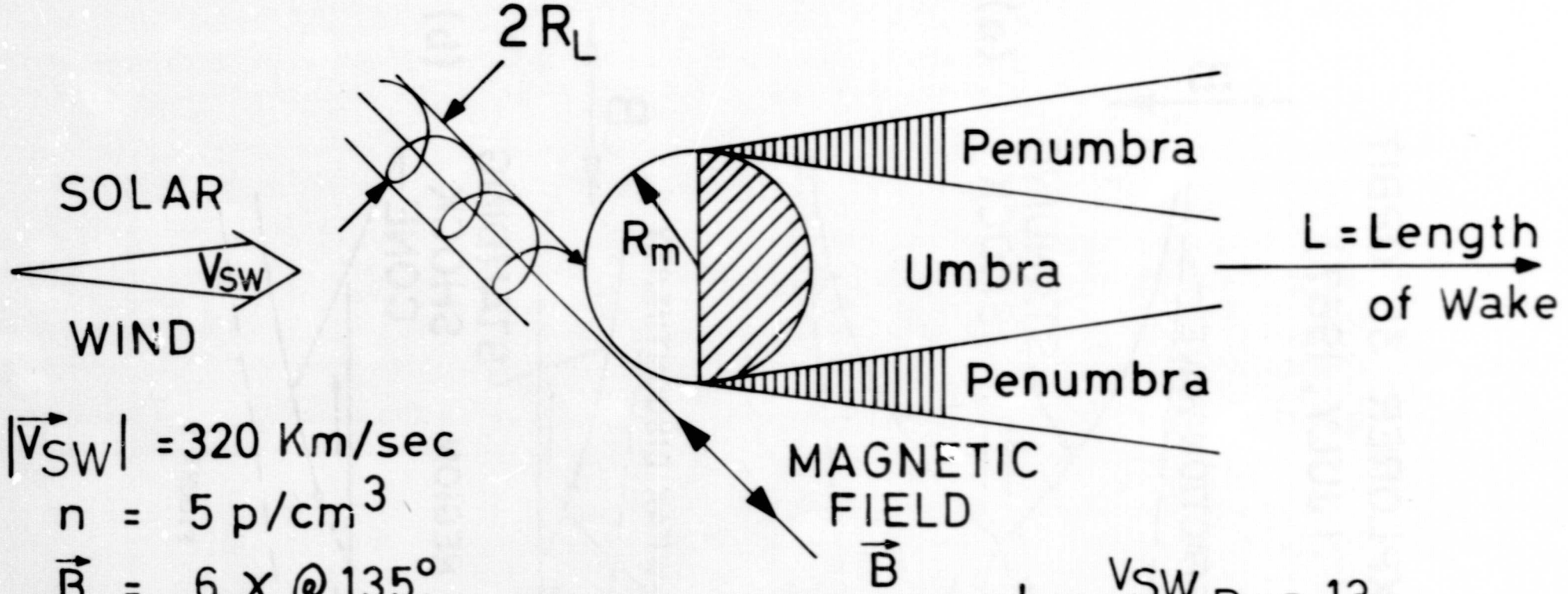

$|\vec{V}_{SW}|$ = 320 Km/sec

n = 5 p/cm^3

$\vec{B}$ = 6 γ @ 135°, 315°

	ions	electrons	Notes
T (°K)	4×10^4	10^5	$T_{///}/T_{\perp}>1$
V_T(Km/sec)	25	1700	
R_L (Km)	44	1.6	R_m=1738
τ_L (sec)	11	6×10^{-3}	

$$L \propto \frac{V_{SW}}{V_{T_i}} R_m = 13$$

$$\tau \propto \frac{2R_m}{V_{SW}} = 11 \text{ sec}$$

$$\beta = \frac{nK(T_e+T_i)}{H^2/8\pi} \approx 1$$

$$V_A = \frac{H}{\sqrt{4\pi n m_i}} = 60 \text{ km/sec}$$

FIGURE 5

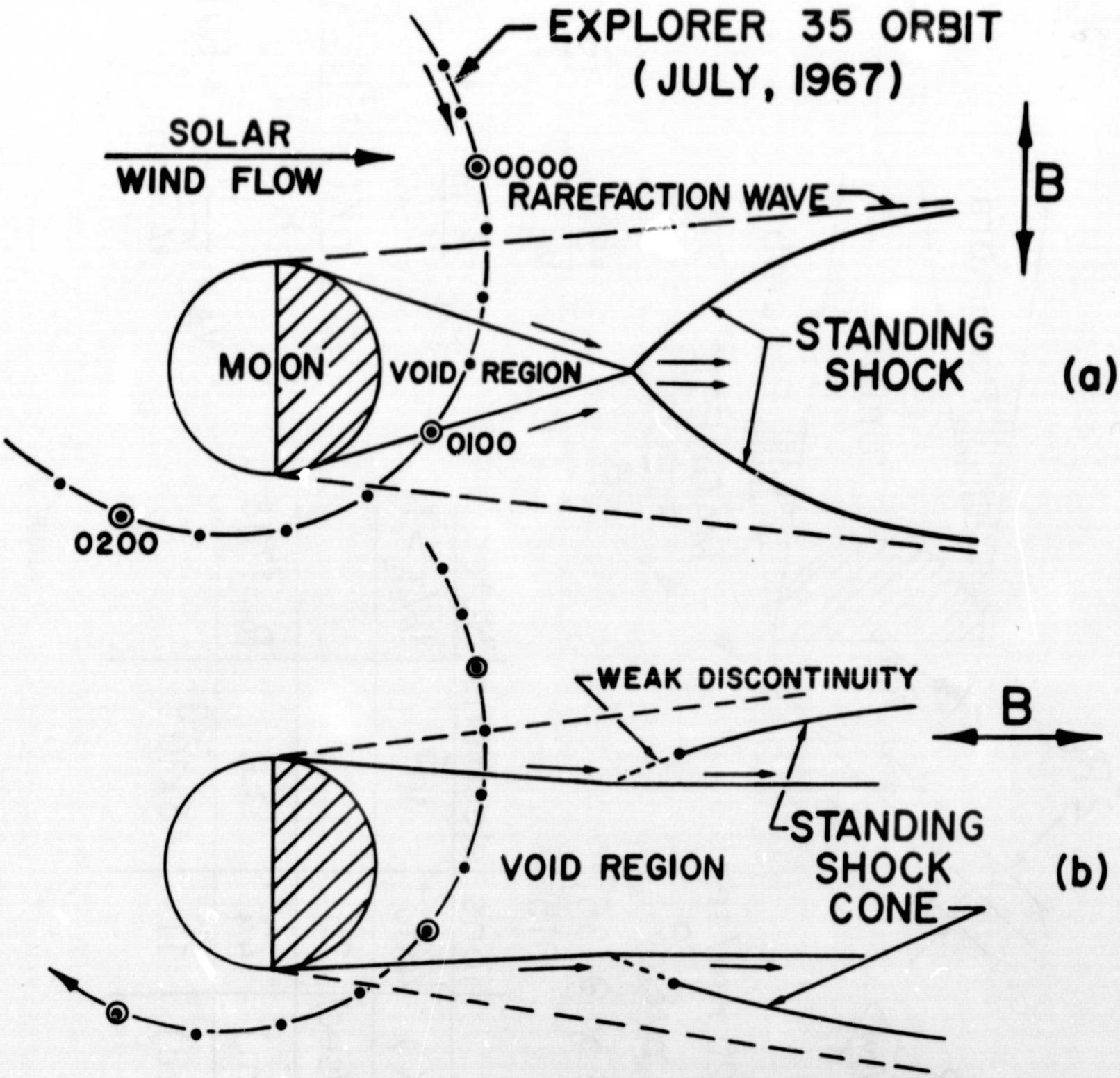
EXPLORER 35 ORBIT
(JULY, 1967)
SOLAR
WIND FLOW
0000
RAREFACTION WAVE
B
MOON
VOID REGION
STANDING
SHOCK
(a)
0100
0200
WEAK DISCONTINUITY
B
STANDING
SHOCK
CONE
VOID REGION
(b)

FIGURE 6

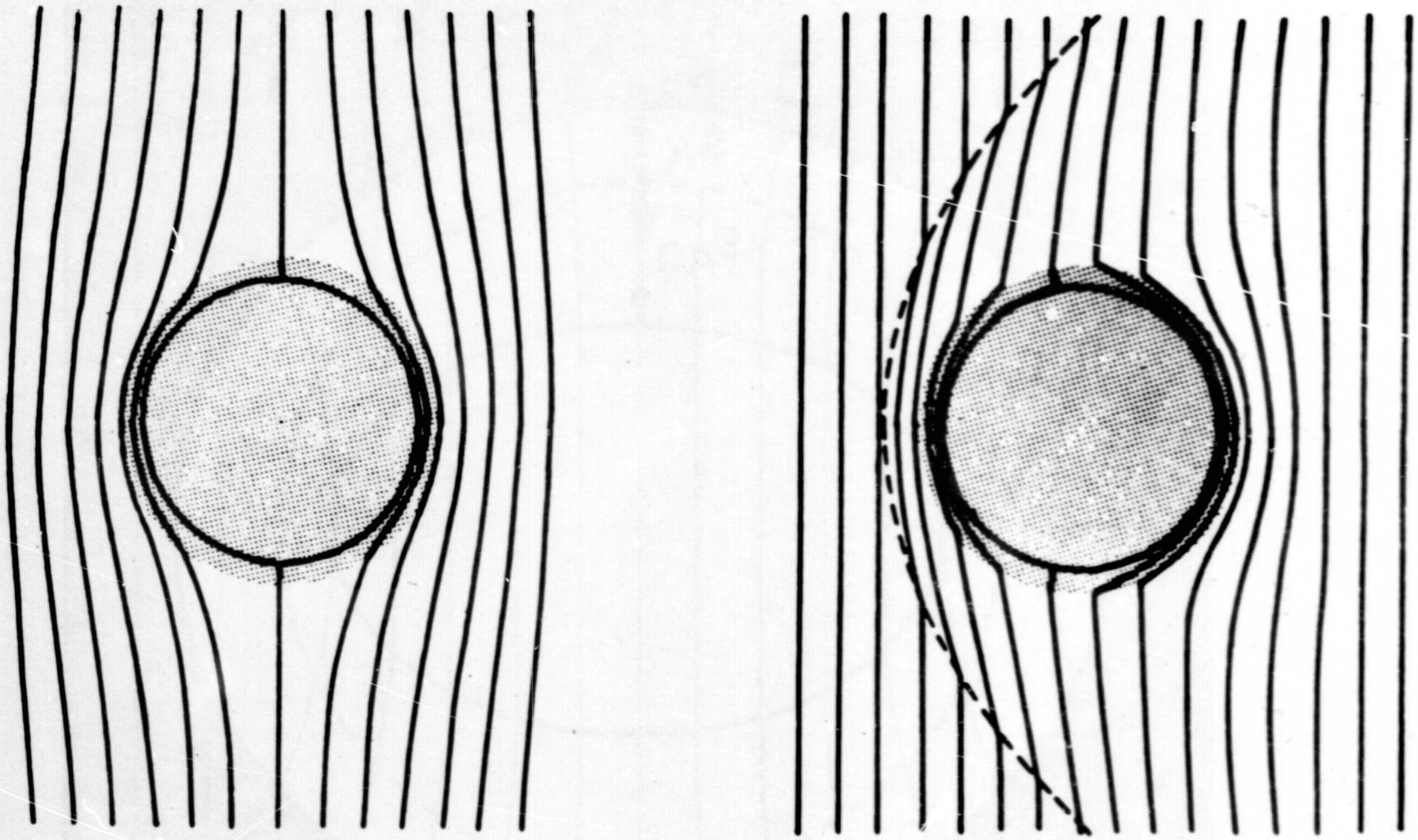

FIGURE 7

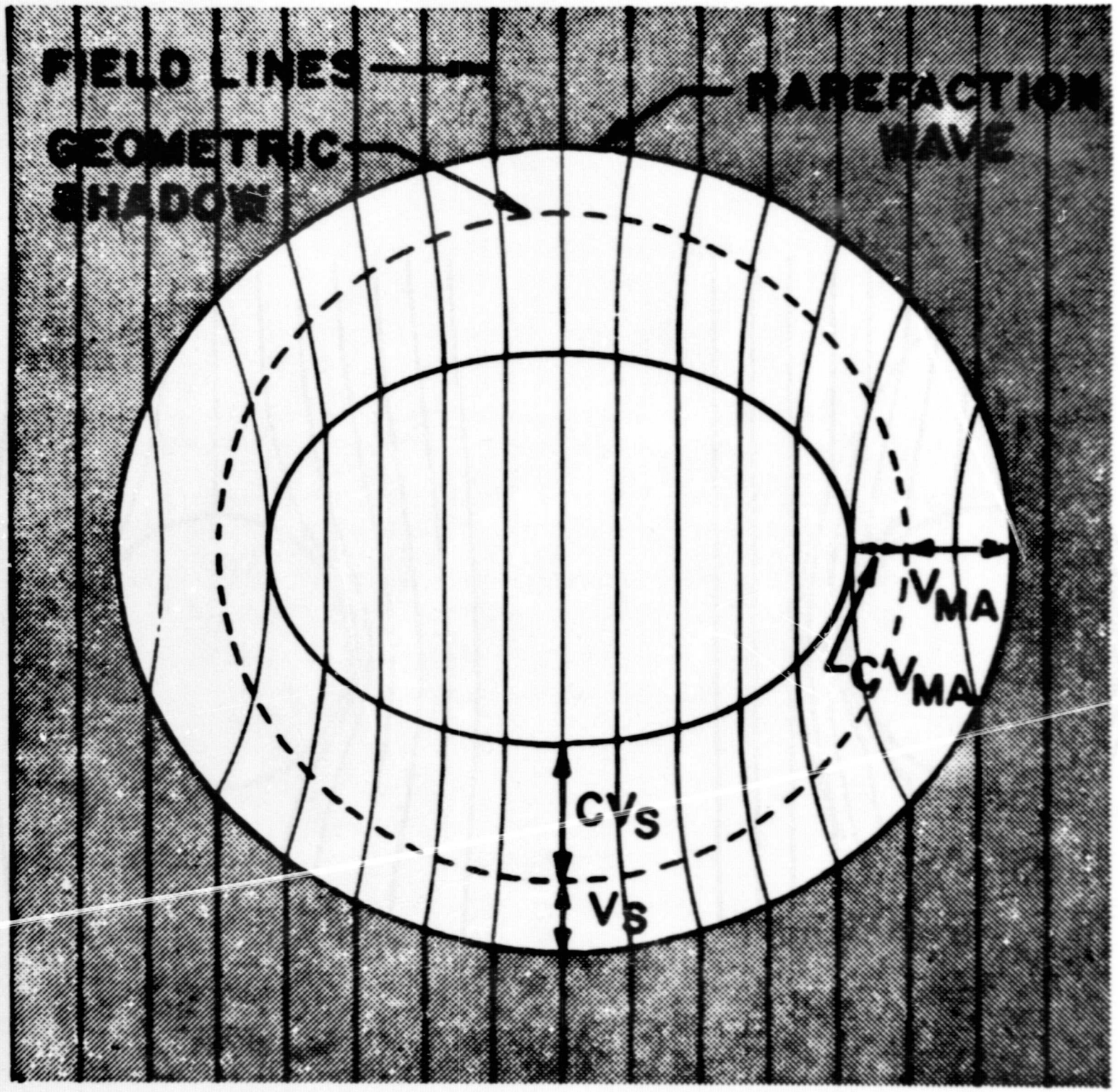
FIELD LINES
GEOMETRIC
SHADOW
RAREFACTION
WAVE
V_{MA}
cV_{MA}
cV_S
V_S

FIGURE 8

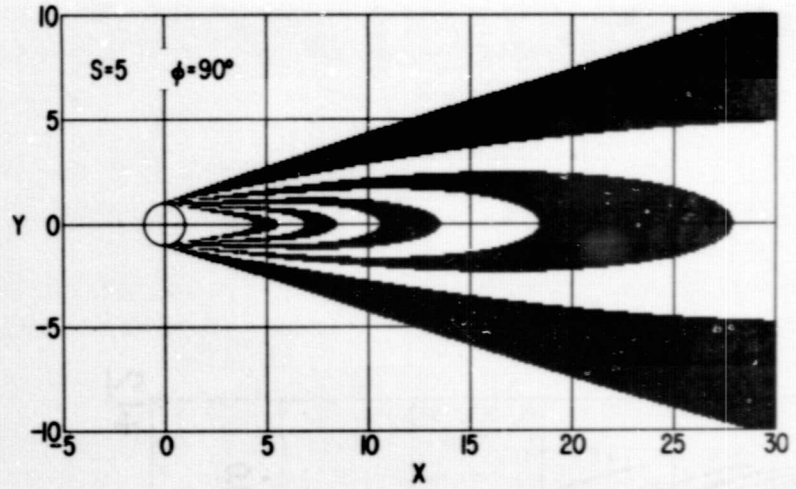
S=5 ϕ=90°
10
5
0
-5
-10
Y
-5 0 5 10 15 20 25 30
X

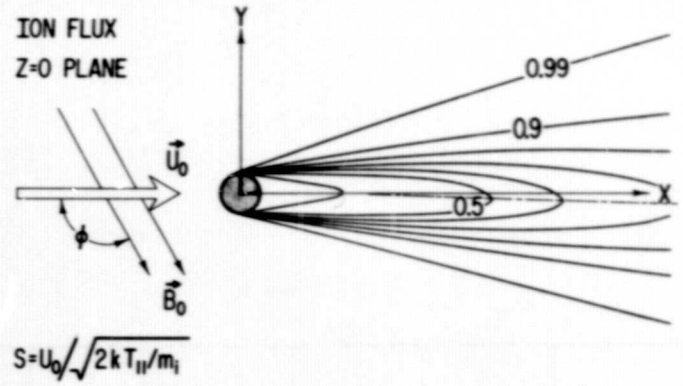
ION FLUX
Z=0 PLANE
$\vec{U}_0$
ϕ
$\vec{B}_0$
Y
0.99
0.9
0.5
X
$S=U_0/\sqrt{2kT_{\parallel}/m_i}$

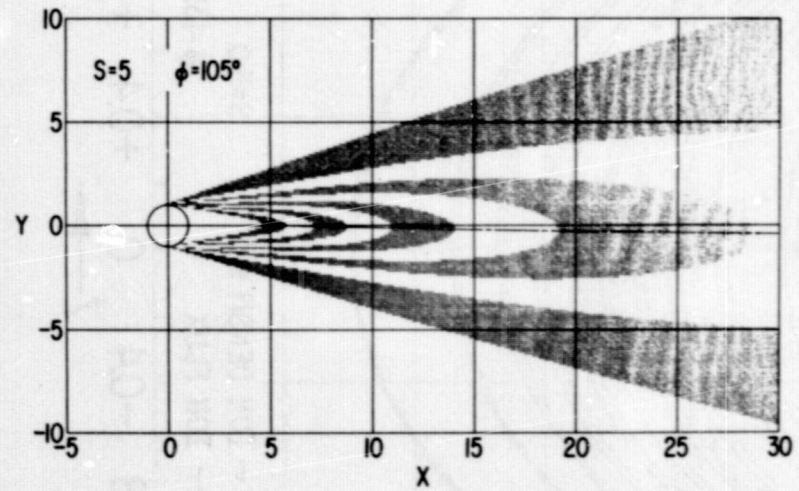
S=5 ϕ=105°
10
5
0
-5
-10
Y
-5 0 5 10 15 20 25 30
X

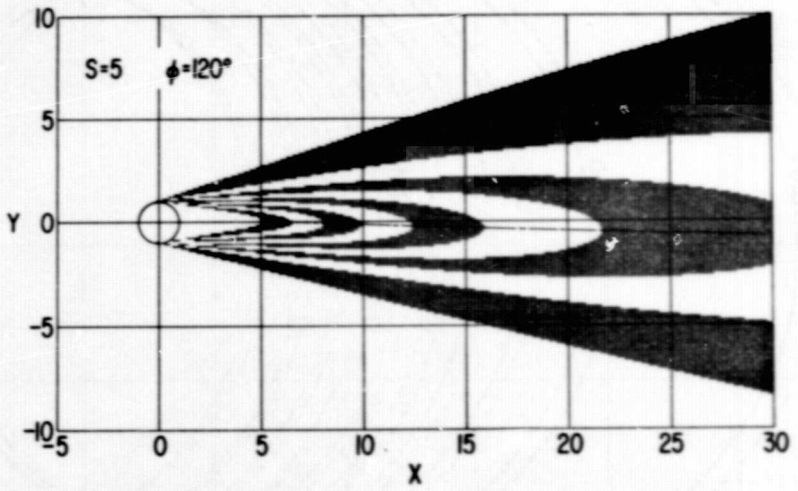
S=5 ϕ=120°
10
5
0
-5
-10
Y
-5 0 5 10 15 20 25 30
X

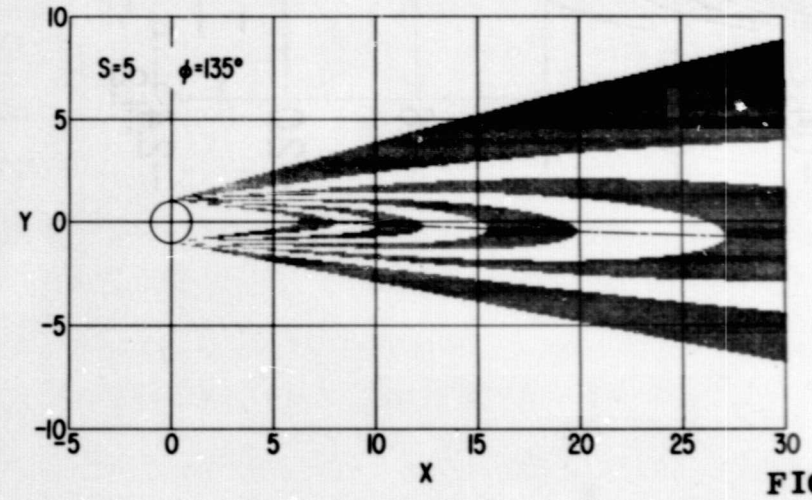
S=5 ϕ=135°
10
5
0
-5
-10
Y
-5 0 5 10 15 20 25 30
X

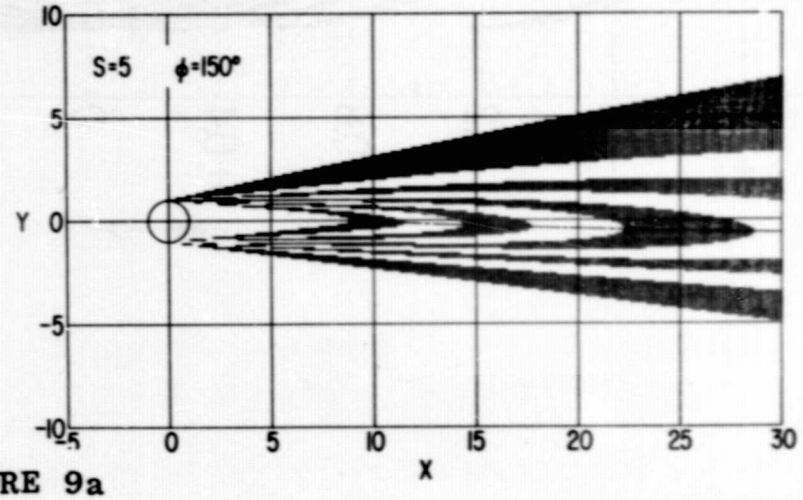
S=5 ϕ=150°
10
5
0
-5
-10
Y
-5 0 5 10 15 20 25 30
X

FIGURE 9a

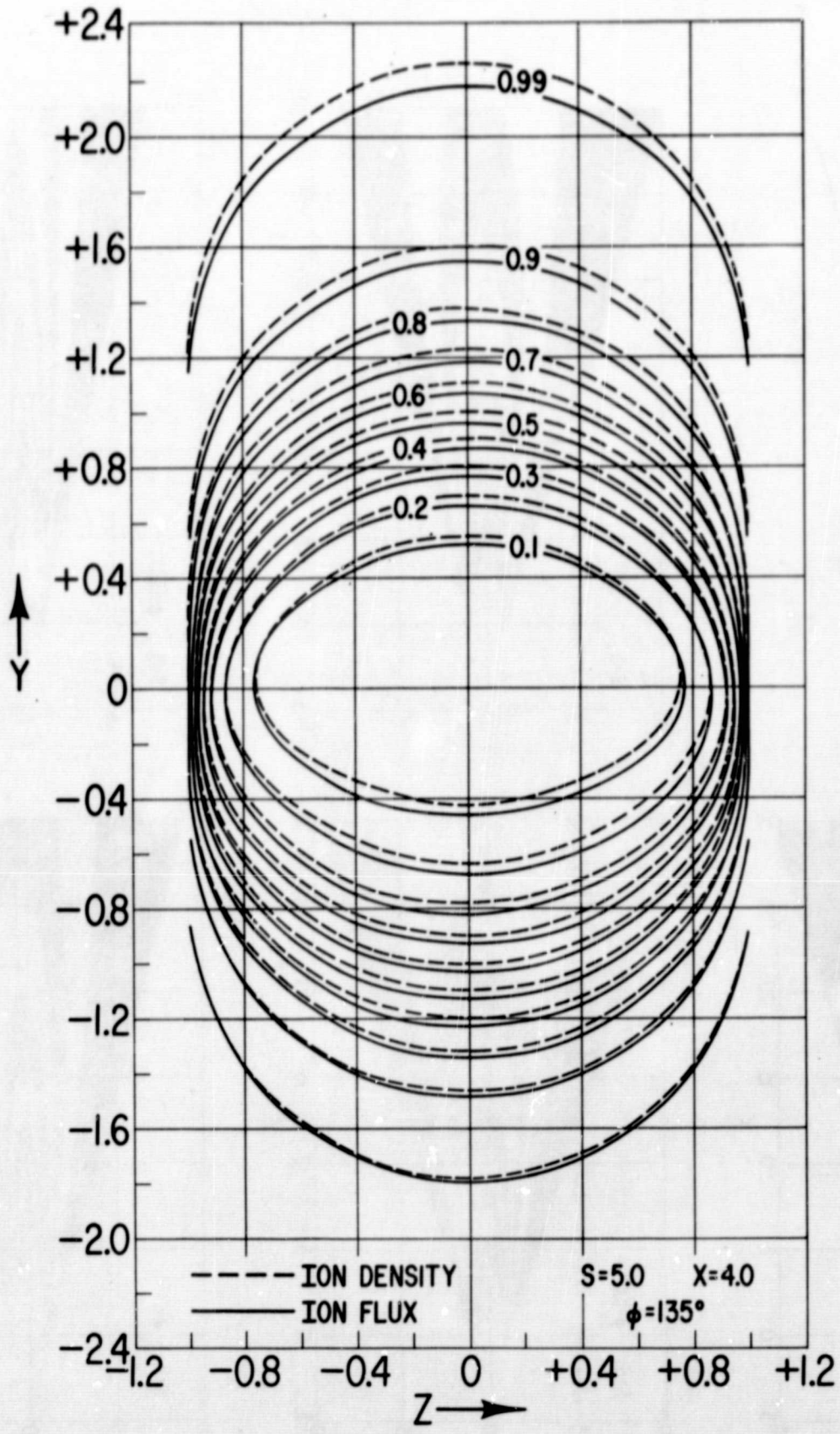
+2.4
+2.0
+1.6
+1.2
+0.8
+0.4
0
−0.4
−0.8
−1.2
−1.6
−2.0
−2.4
0.99
0.9
0.8
0.7
0.6
0.5
0.4
0.3
0.2
0.1
Y
Z
−1.2
−0.8
−0.4
0
+0.4
+0.8
+1.2
ION DENSITY
ION FLUX
S=5.0
X=4.0
φ=135°

FIGURE 9b

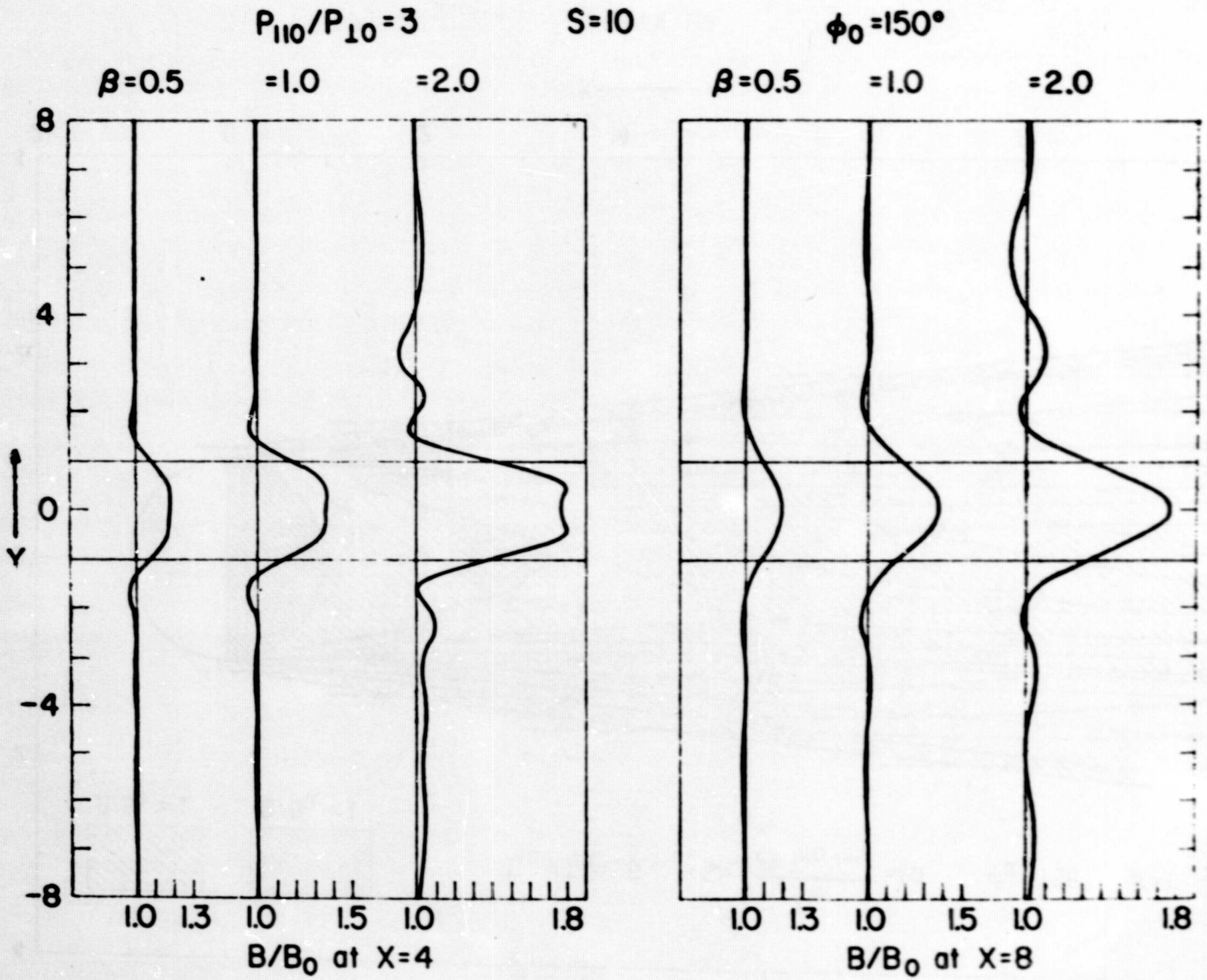
$P_{110}/P_{\perp 0}=3$
S=10
$\phi_0=150°$
β=0.5
=1.0
=2.0
8
4
0
-4
-8
Y
1.0 1.3 1.0 1.5 1.0 1.8
B/B_0 at X=4
B/B_0 at X=8

FIGURE 10[a]

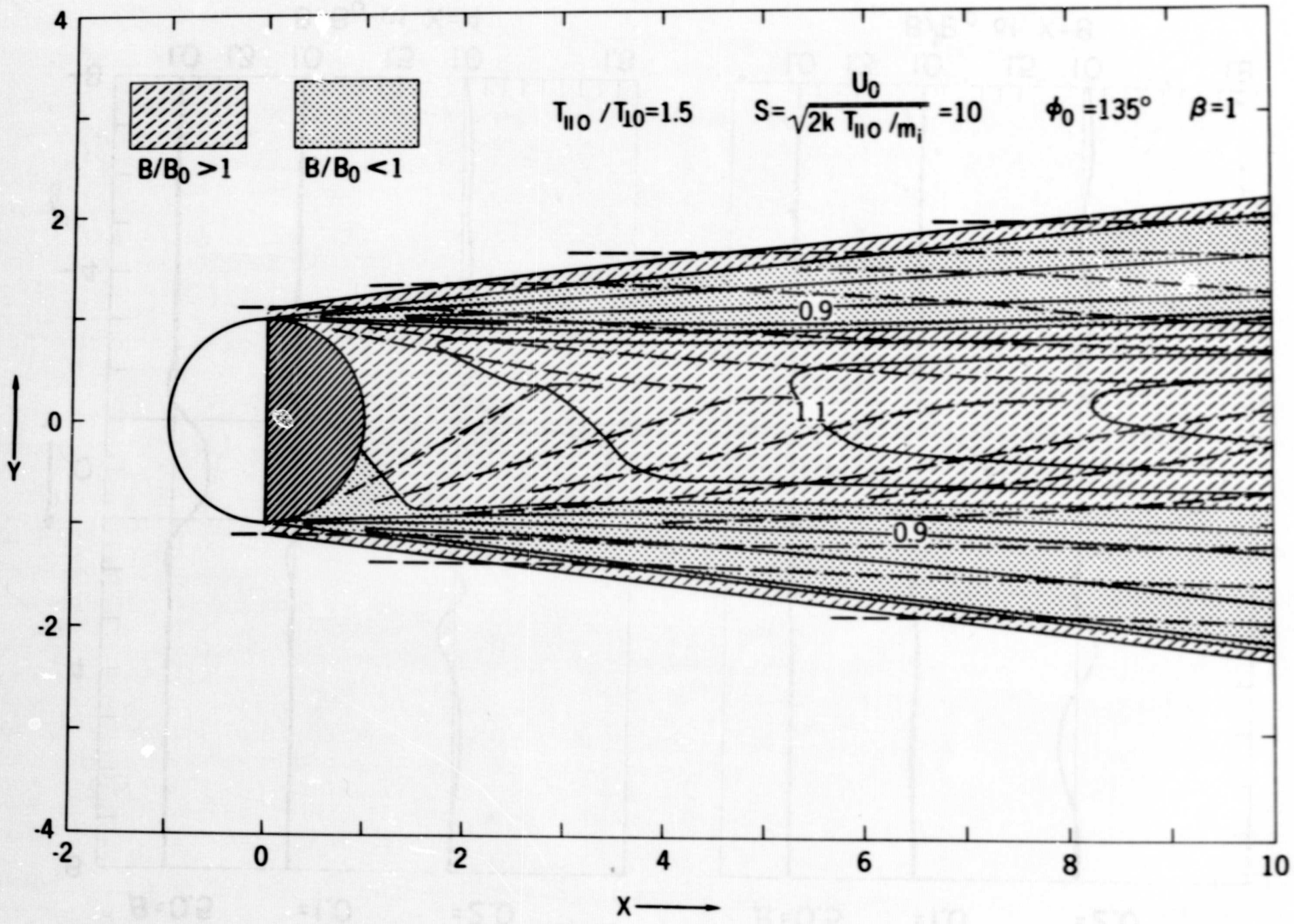
$T_{\parallel 0}/T_{\perp 0}=1.5$
$S=\frac{U_0}{\sqrt{2k\,T_{\parallel 0}/m_i}}=10$
$\phi_0=135°$
$\beta=1$
$B/B_0>1$
$B/B_0<1$
0.9
1.1
0.9
Y
X
4
2
0
-2
-4
-2
0
2
4
6
8
10

FIGURE 10b

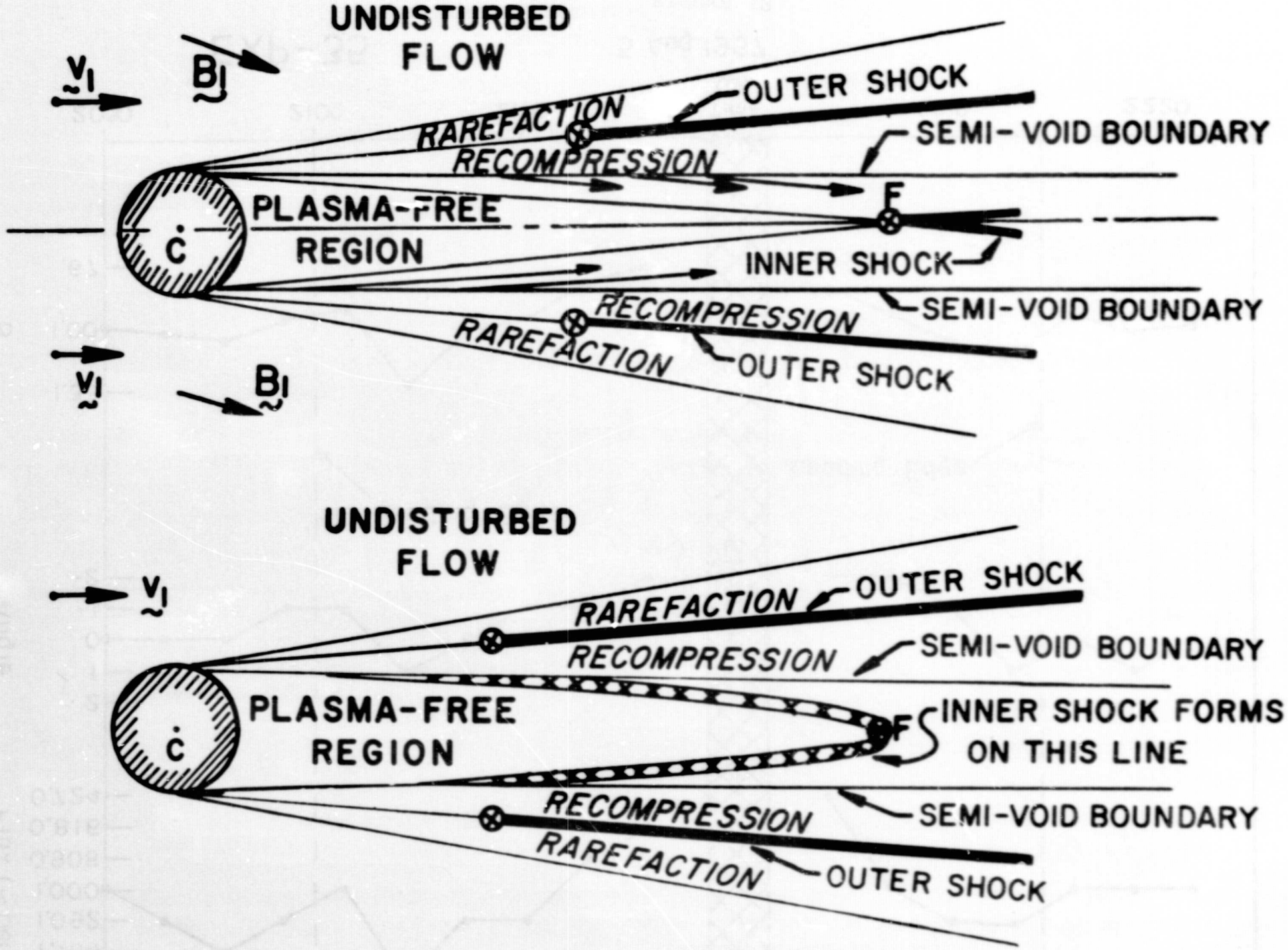
UNDISTURBED
FLOW
V_I
B_I
RAREFACTION
OUTER SHOCK
SEMI-VOID BOUNDARY
RECOMPRESSION
F
PLASMA-FREE
REGION
C
INNER SHOCK
SEMI-VOID BOUNDARY
RECOMPRESSION
RAREFACTION
OUTER SHOCK
V_I
B_I
UNDISTURBED
FLOW
V_I
RAREFACTION
OUTER SHOCK
RECOMPRESSION
SEMI-VOID BOUNDARY
PLASMA-FREE
REGION
C
F
INNER SHOCK FORMS
ON THIS LINE
RECOMPRESSION
SEMI-VOID BOUNDARY
RAREFACTION
OUTER SHOCK

FIGURE 11

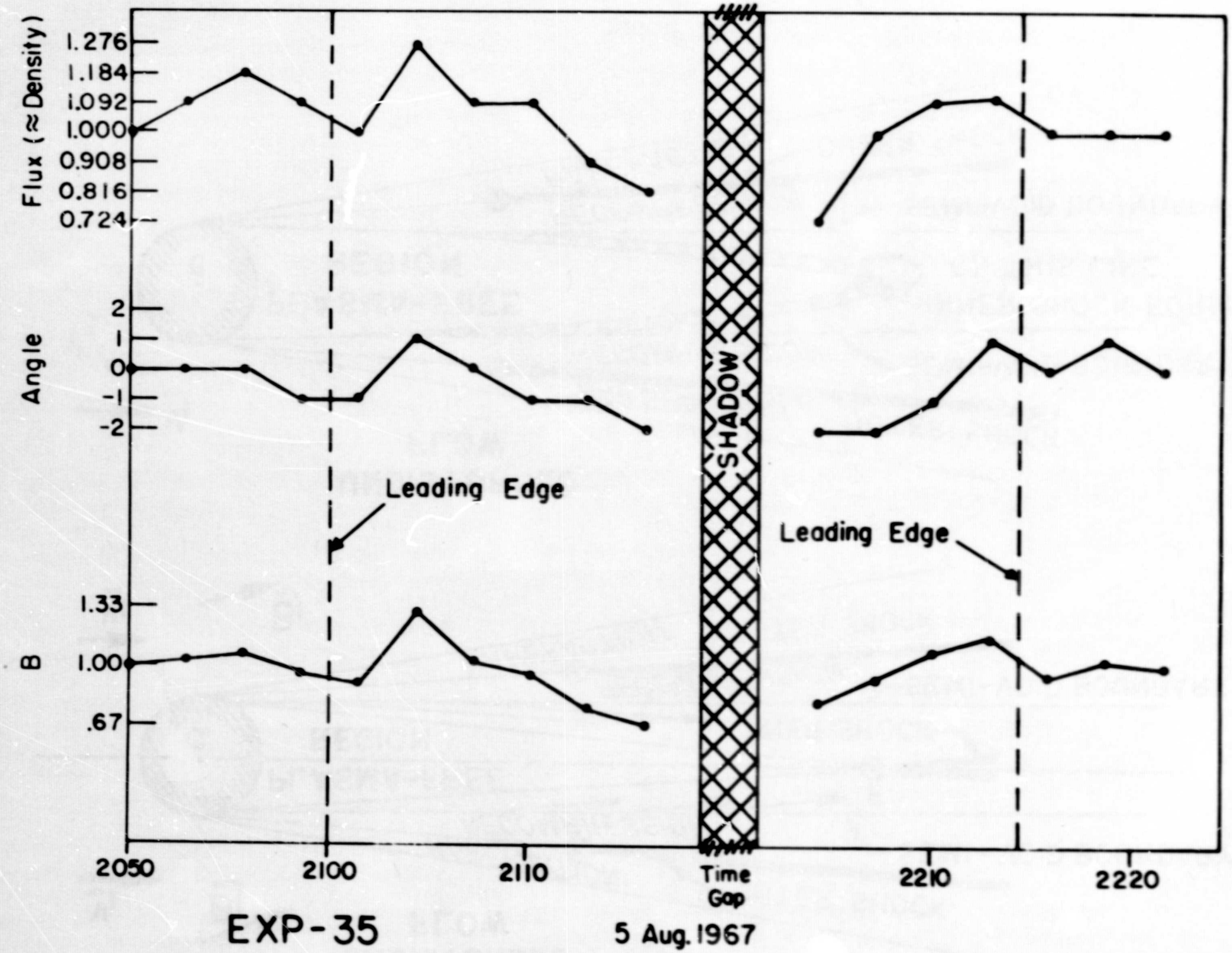

EXP-35

5 Aug. 1967

FIGURE 12

FIELD LINE THREADING OF MOON

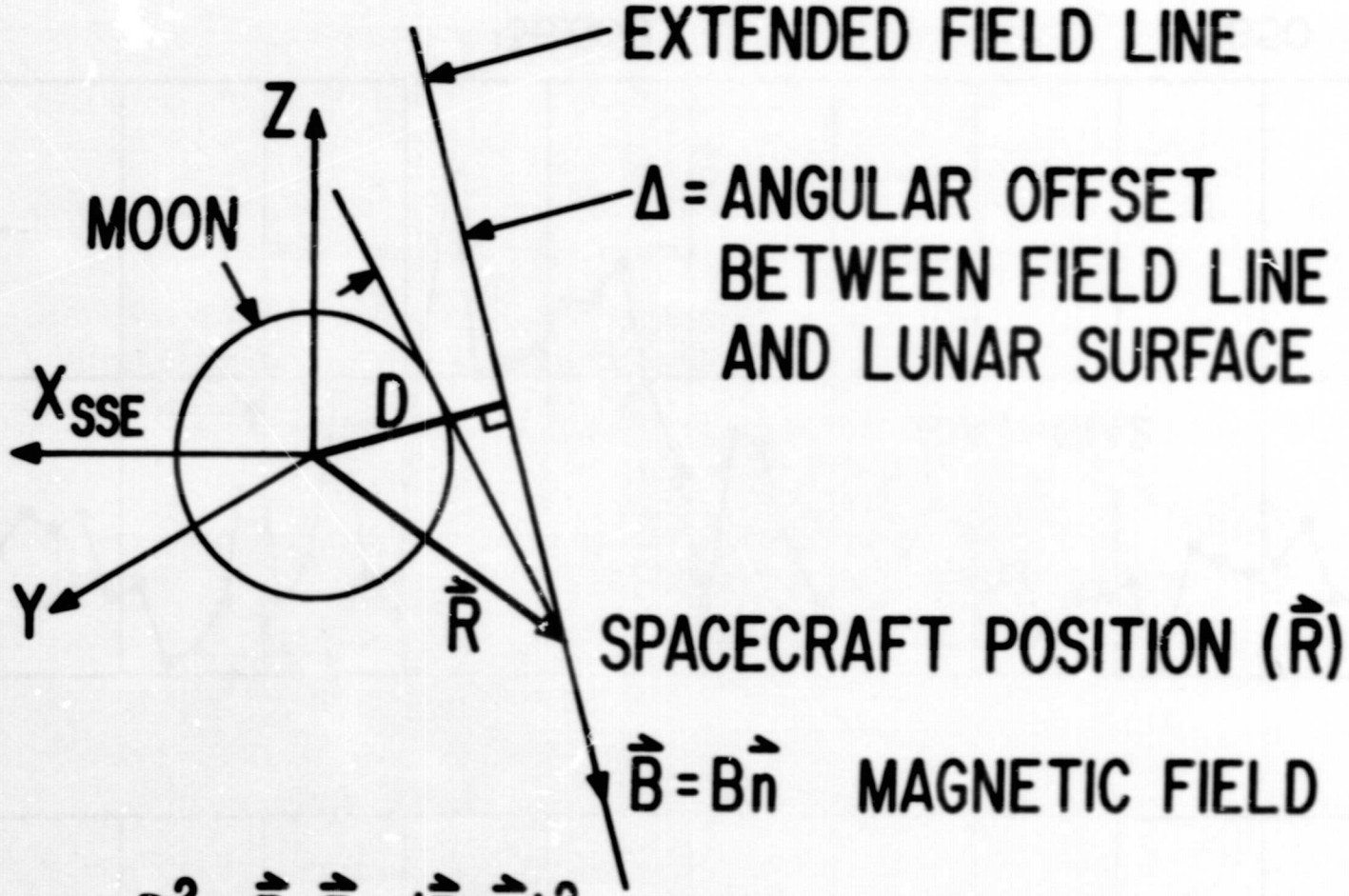

$$D^2 = \vec{R}\cdot\vec{R} - (\vec{R}\cdot\vec{n})^2$$

$$\Delta = \tan^{-1}\left(D/|\vec{R}\cdot\vec{n}|\right) - \tan^{-1}\left(1/\sqrt{R^2-1}\right)$$

FIGURE 13a

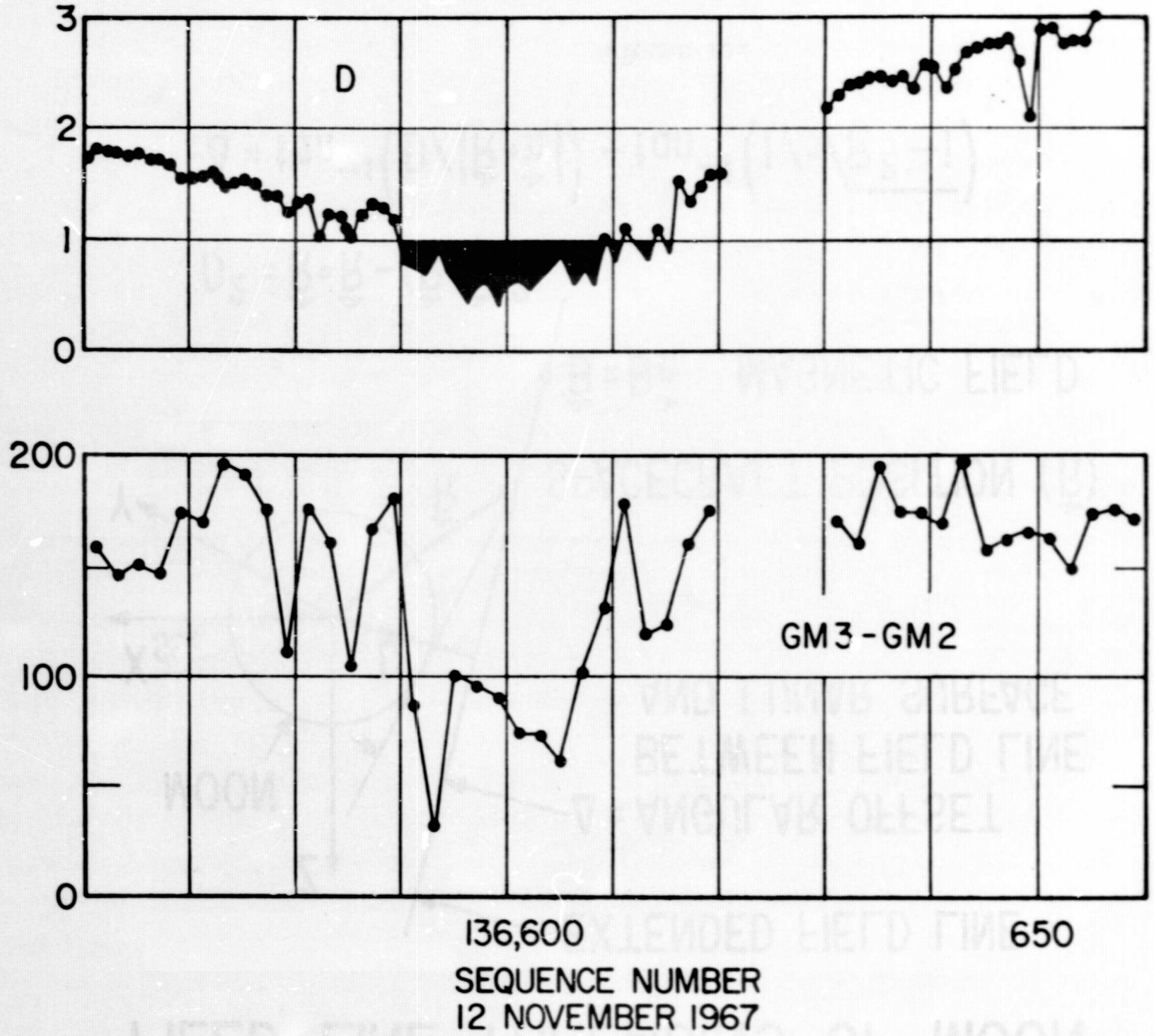
3
2
1
0
D
200
100
0
GM3-GM2
136,600
650
SEQUENCE NUMBER
12 NOVEMBER 1967

FIGURE 13b

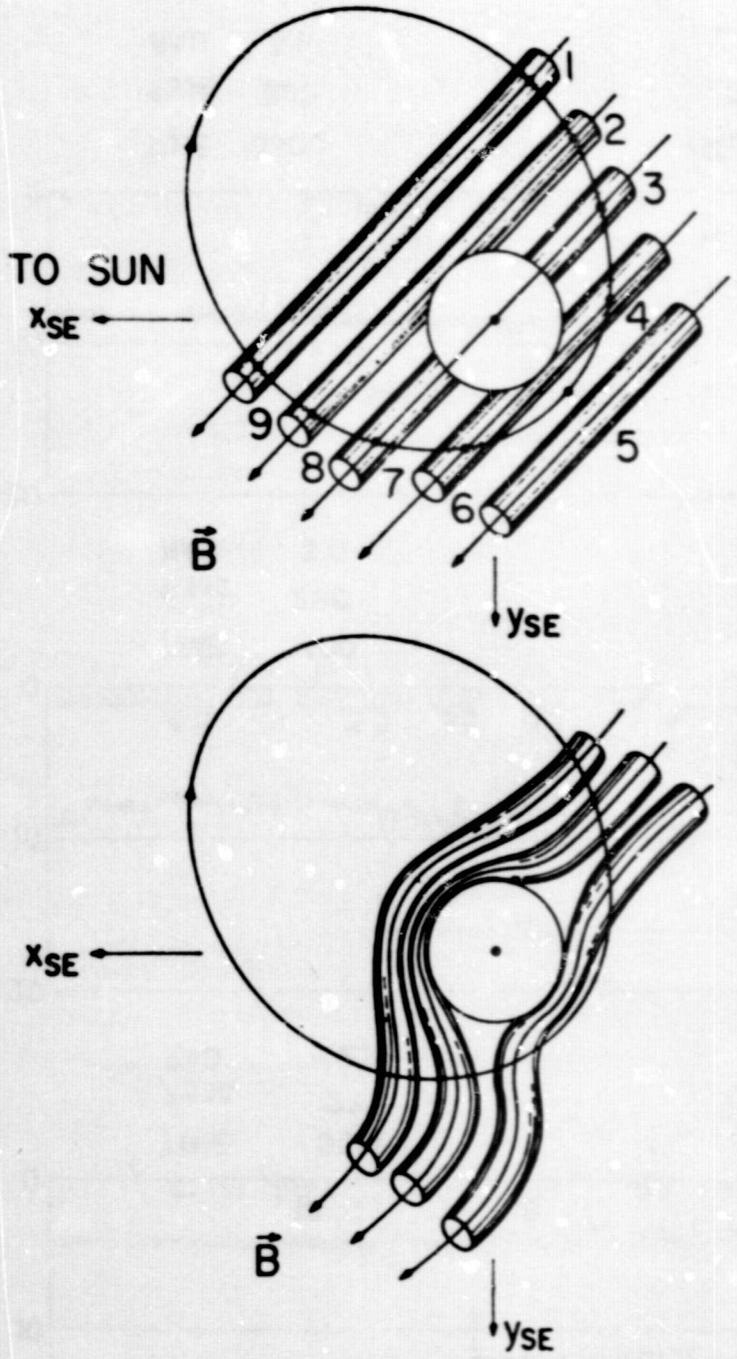

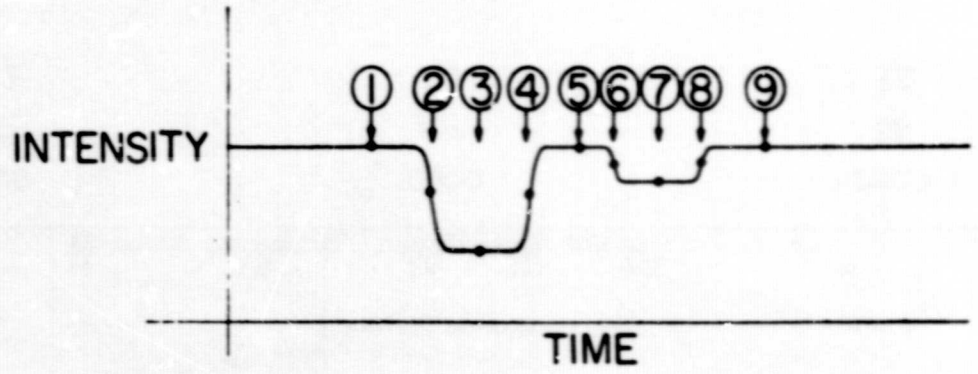

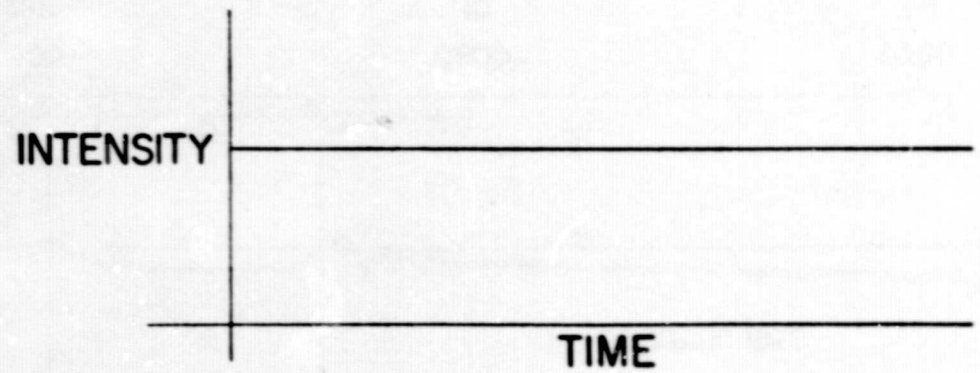

50 KEV ELECTRON SHADOWING
BY THE MOON - SCHEMATIC

FIGURE 14

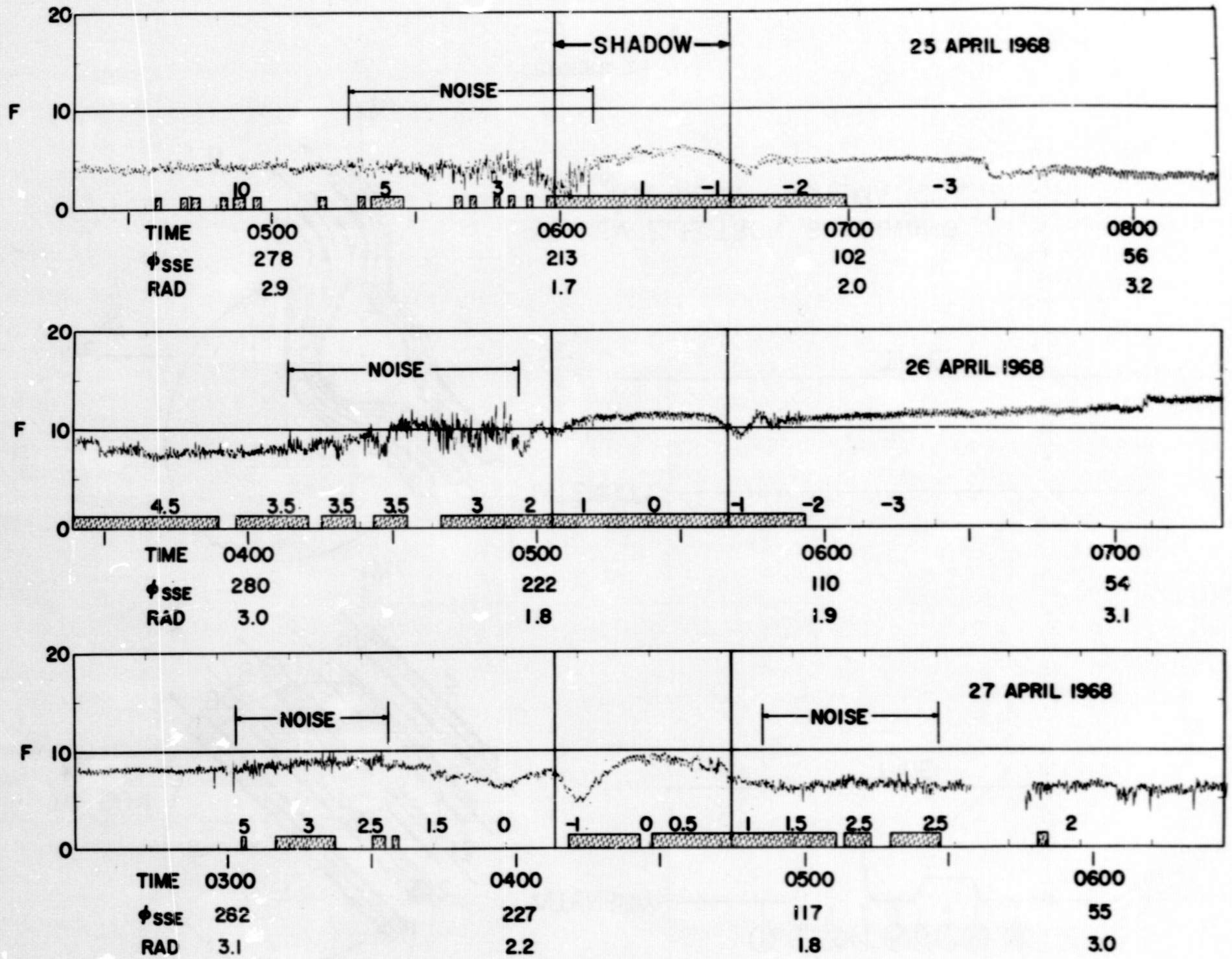
20
F 10
0
SHADOW
25 APRIL 1968
NOISE
10
5
3
1
-1
-2
-3
TIME 0500 0600 0700 0800
ϕSSE 278 213 102 56
RAD 2.9 1.7 2.0 3.2
20
F 10
0
NOISE
26 APRIL 1968
4.5
3.5
3.5
3.5
3
2
1
0
-1
-2
-3
TIME 0400 0500 0600 0700
ϕSSE 280 222 110 54
RAD 3.0 1.8 1.9 3.1
20
F 10
0
NOISE
27 APRIL 1968
NOISE
5
3
2.5
1.5
0
-1
0
0.5
1
1.5
2.5
2.5
2
TIME 0300 0400 0500 0600
ϕSSE 262 227 117 55
RAD 3.1 2.2 1.8 3.0

FIGURE 15

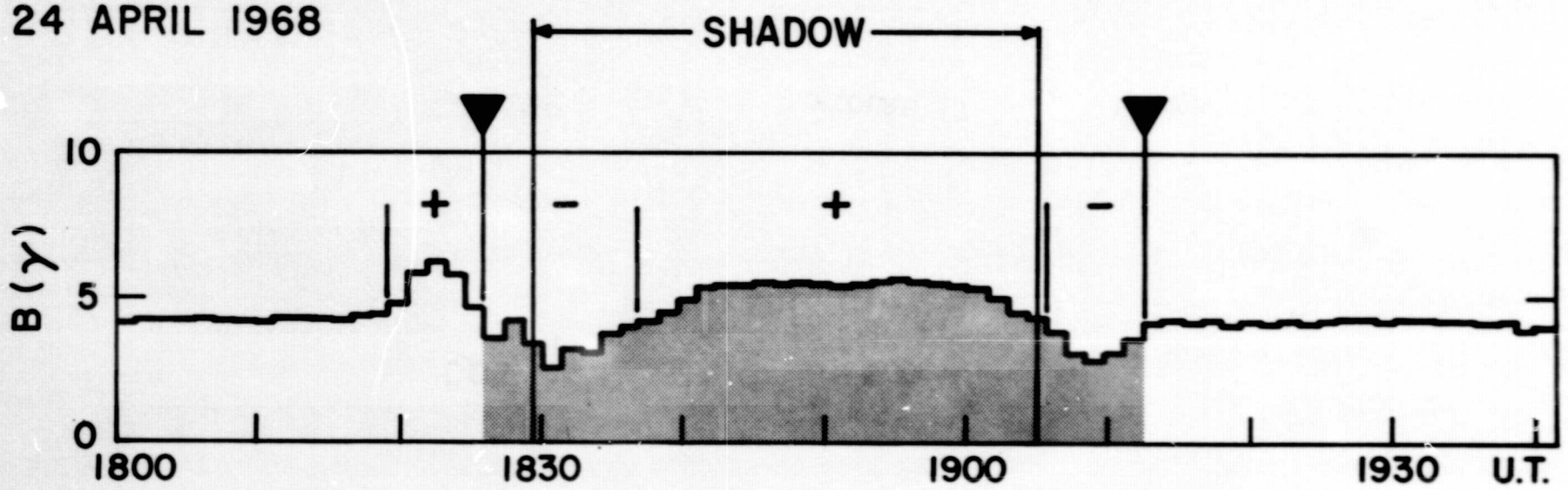

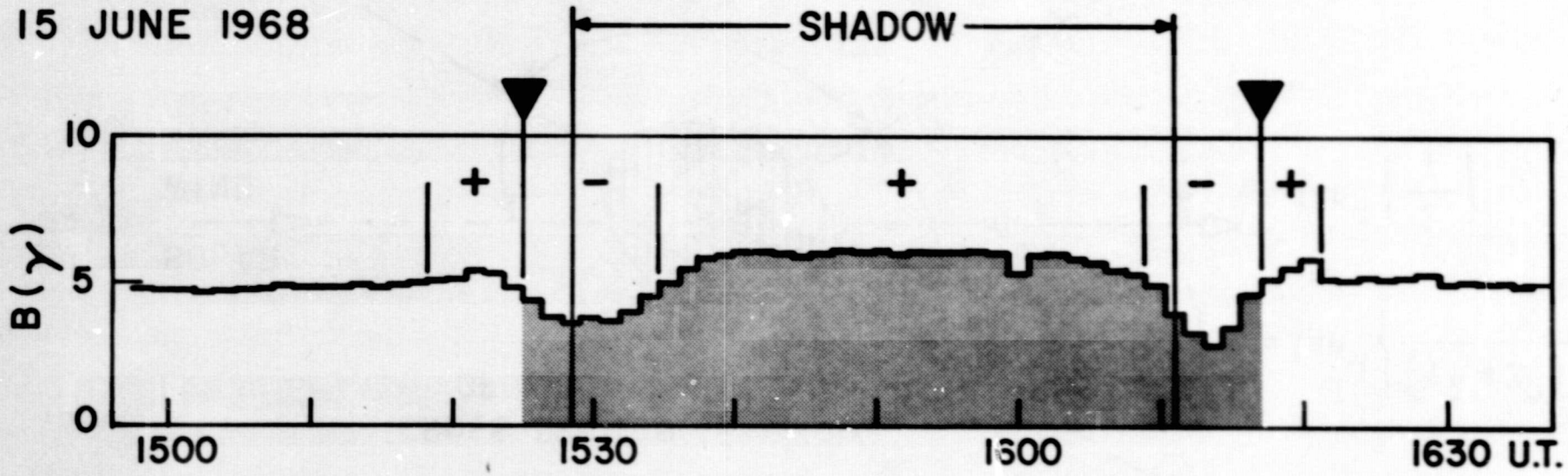

▼ MACH CONE CROSSING

FIGURE 16

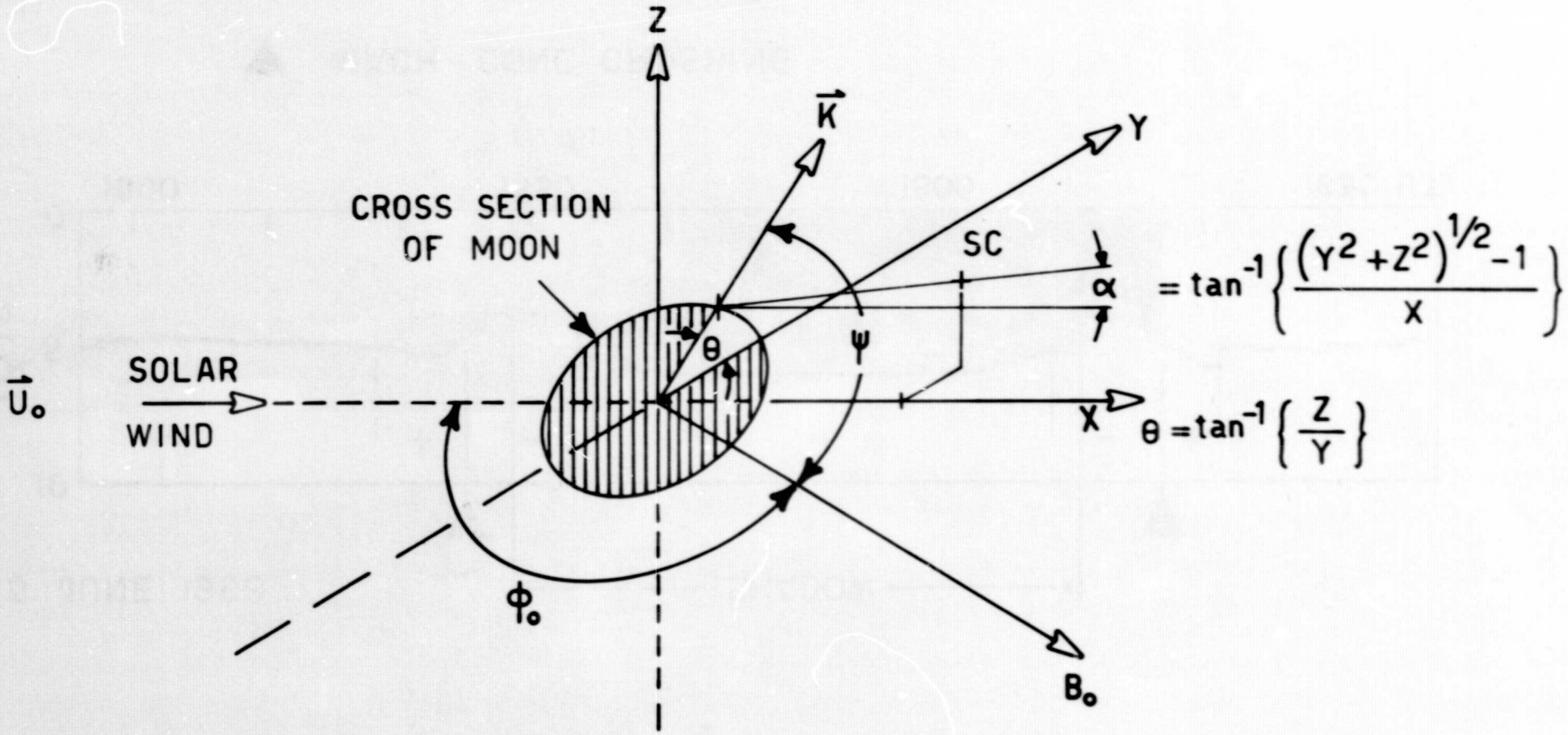

$$\cos \psi \approx \sin \Phi_o \cos \theta$$

FIGURE 17

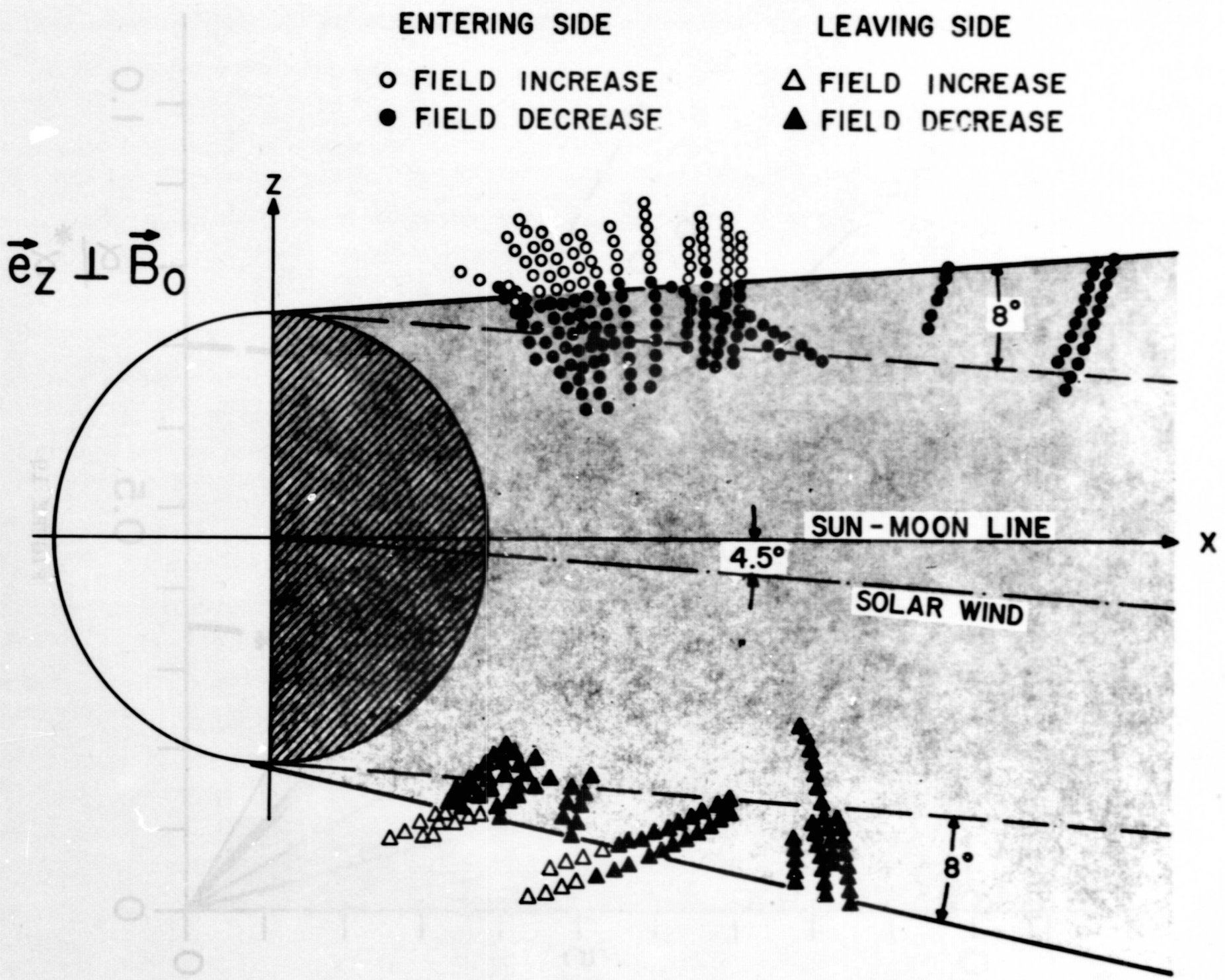
ENTERING SIDE
LEAVING SIDE
FIELD INCREASE
FIELD DECREASE
FIELD INCREASE
FIELD DECREASE
z
$\vec{e}_z \perp \vec{B}_0$
8°
SUN - MOON LINE
4.5°
SOLAR WIND
x
8°

FIGURE 18

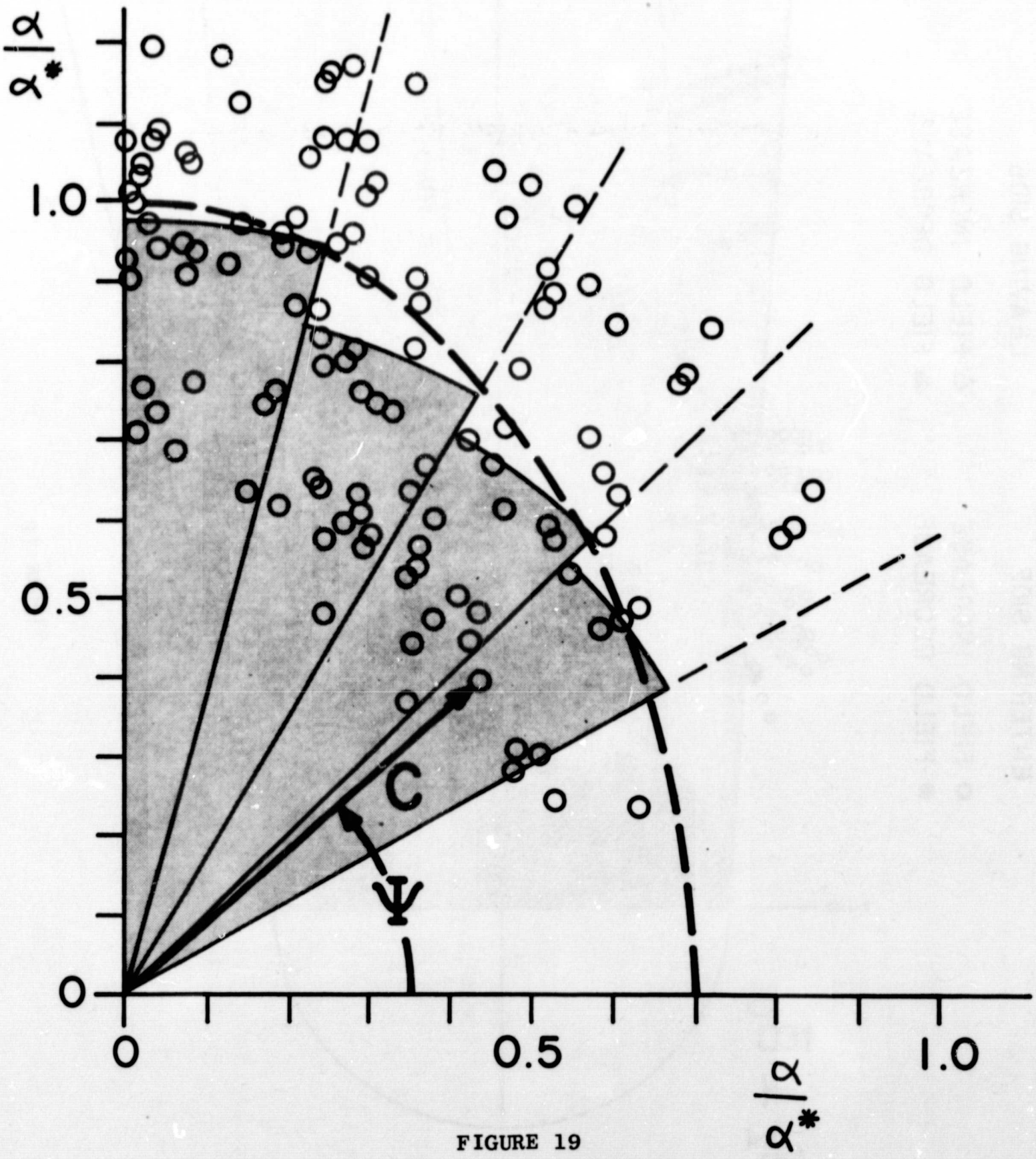

FIGURE 19

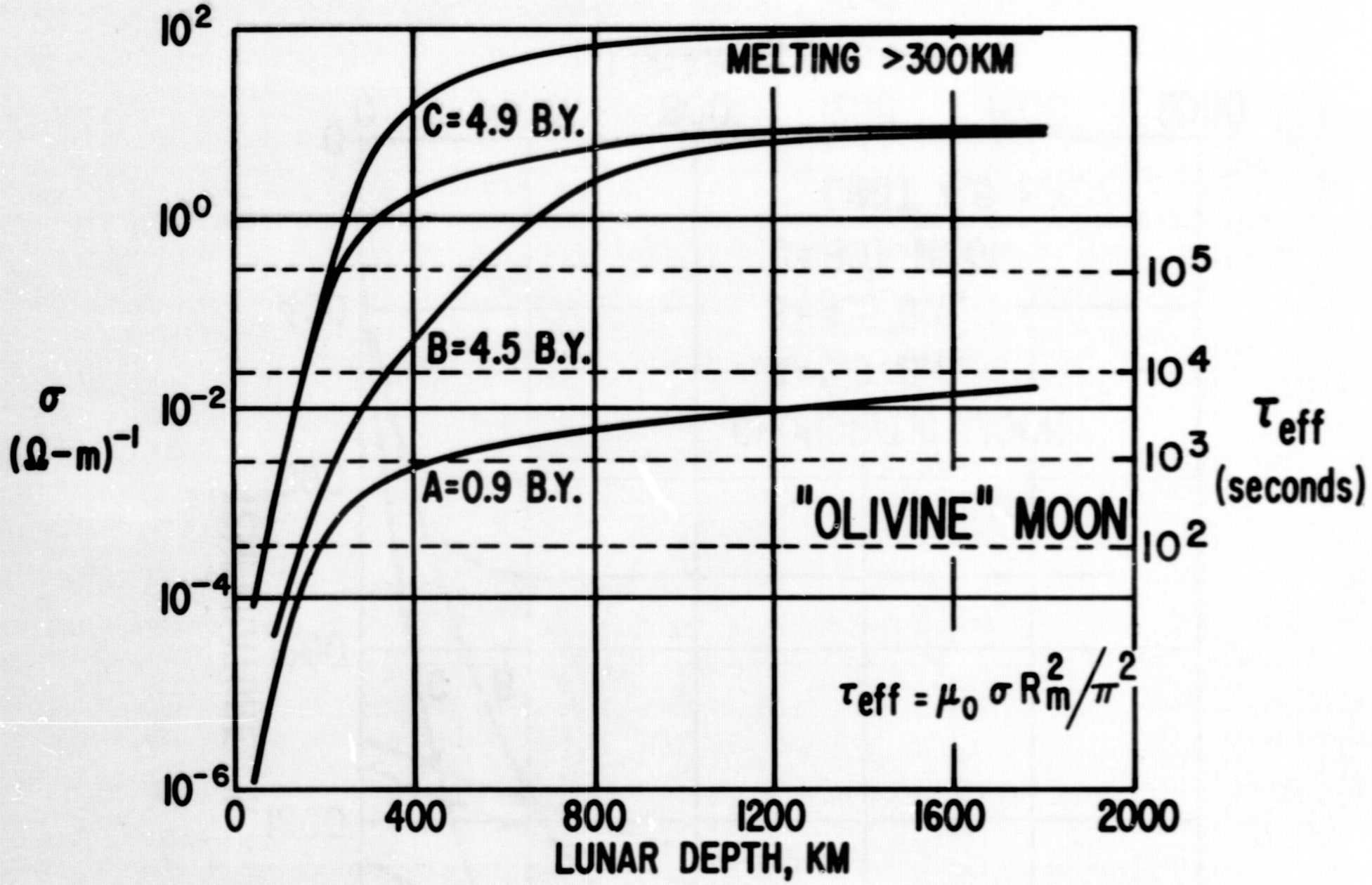
MELTING >300KM
C=4.9 B.Y.
B=4.5 B.Y.
A=0.9 B.Y.
"OLIVINE" MOON
$\tau_{eff} = \mu_0 \sigma R_m^2/\pi^2$
10^2
10^0
10^{-2}
10^{-4}
10^{-6}
σ $(\Omega\text{-m})^{-1}$
10^5
10^4
10^3
10^2
τ_{eff} (seconds)
0
400
800
1200
1600
2000
LUNAR DEPTH, KM

FIGURE 20a

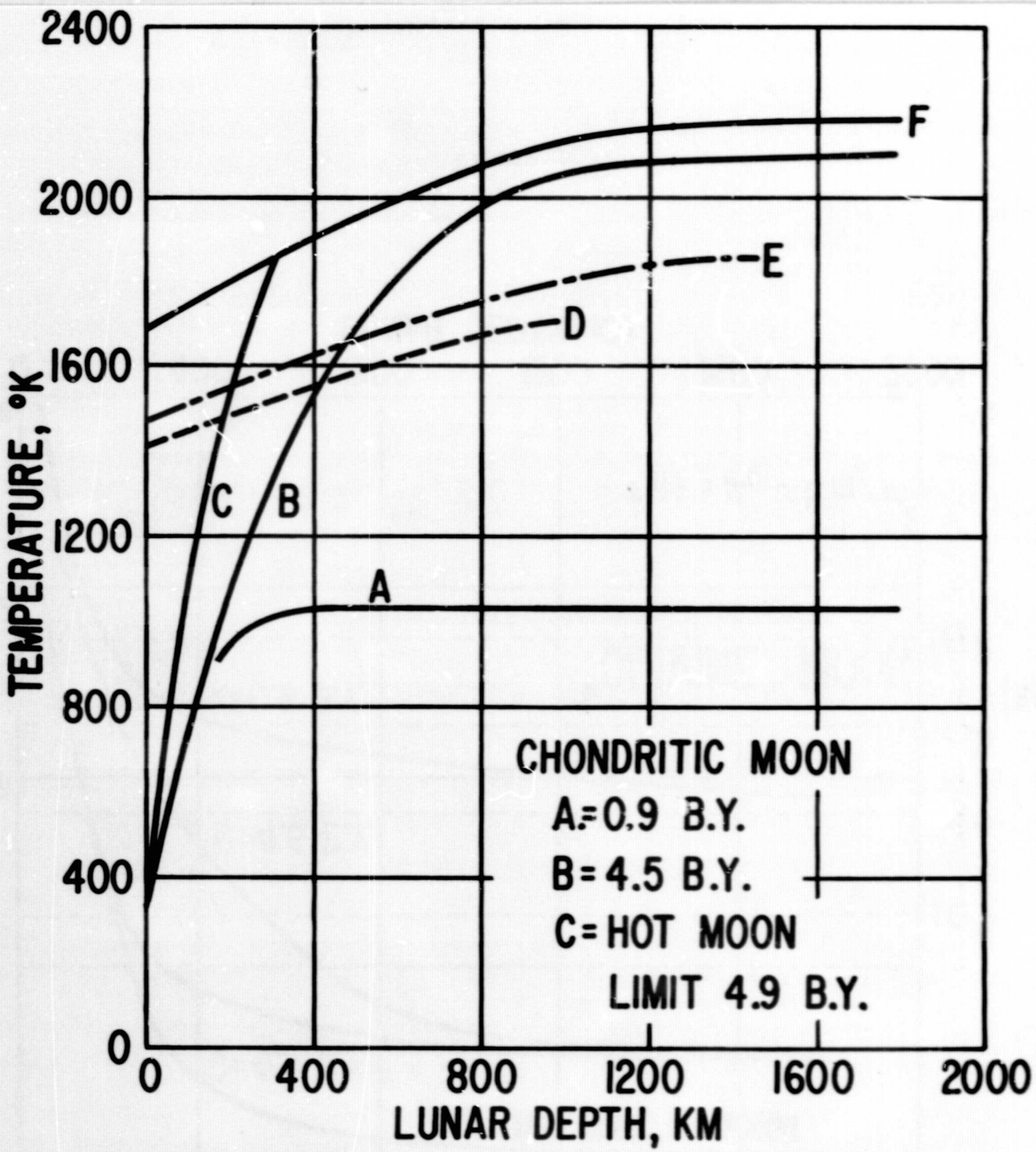
2400
2000
1600
1200
800
400
0
TEMPERATURE, °K
0
400
800
1200
1600
2000
LUNAR DEPTH, KM
A
B
C
D
E
F
CHONDRITIC MOON
A=0.9 B.Y.
B=4.5 B.Y.
C=HOT MOON
LIMIT 4.9 B.Y.

FIGURE 20b

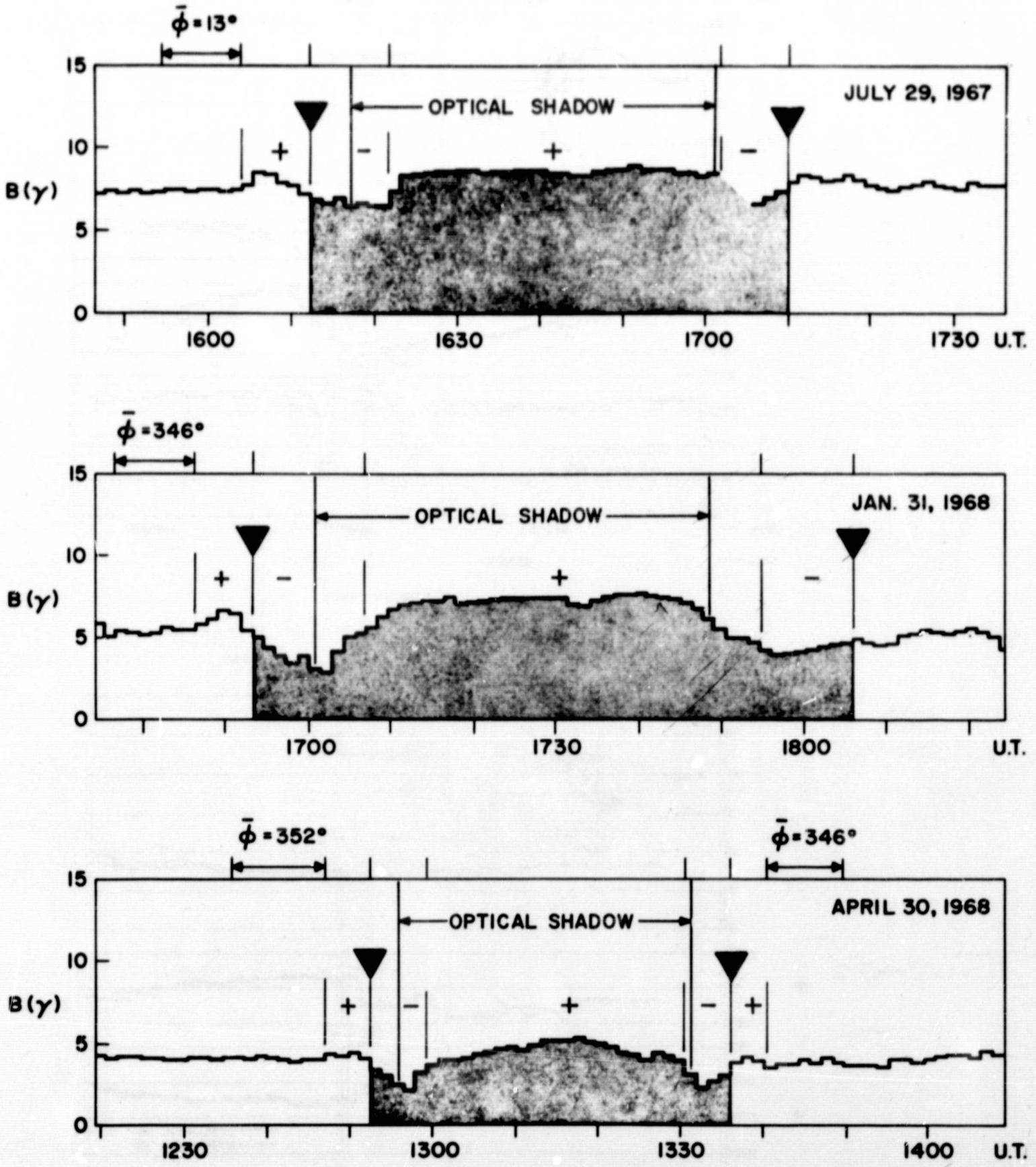
$\bar{\phi}$ = 13°
15
10
5
0
B(γ)
OPTICAL SHADOW
JULY 29, 1967
+
−
+
−
1600
1630
1700
1730 U.T.
$\bar{\phi}$ = 346°
JAN. 31, 1968
1700
1730
1800
U.T.
$\bar{\phi}$ = 352°
$\bar{\phi}$ = 346°
APRIL 30, 1968
1230
1300
1330
1400
U.T.

FIGURE 21

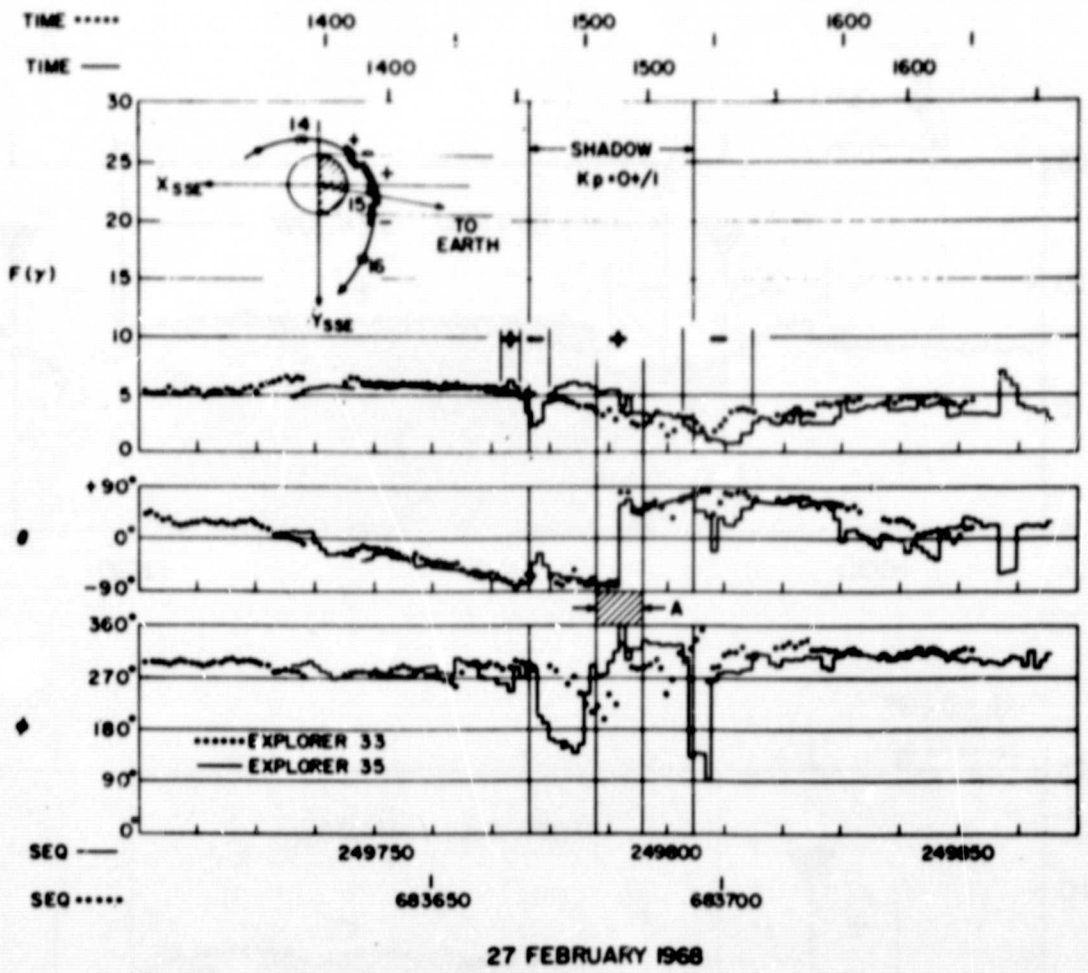

27 FEBRUARY 1968

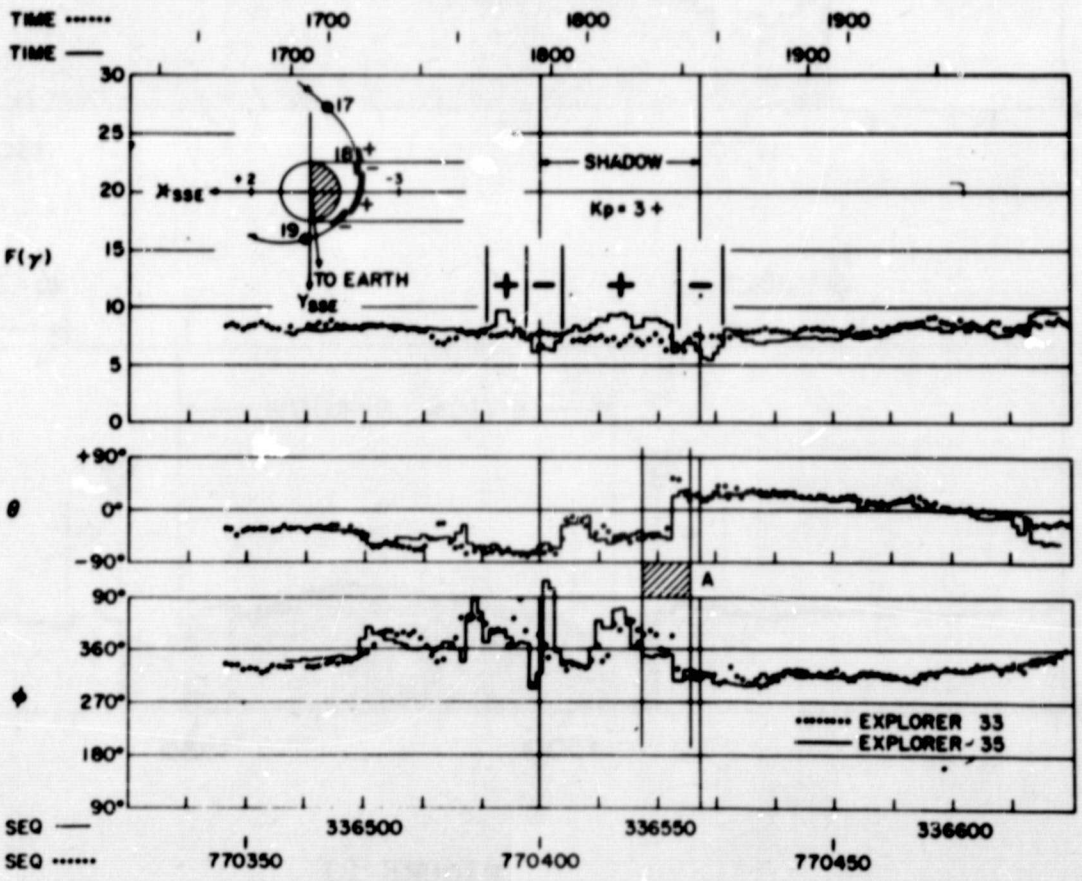

19 MAY 1968

FIGURE 22

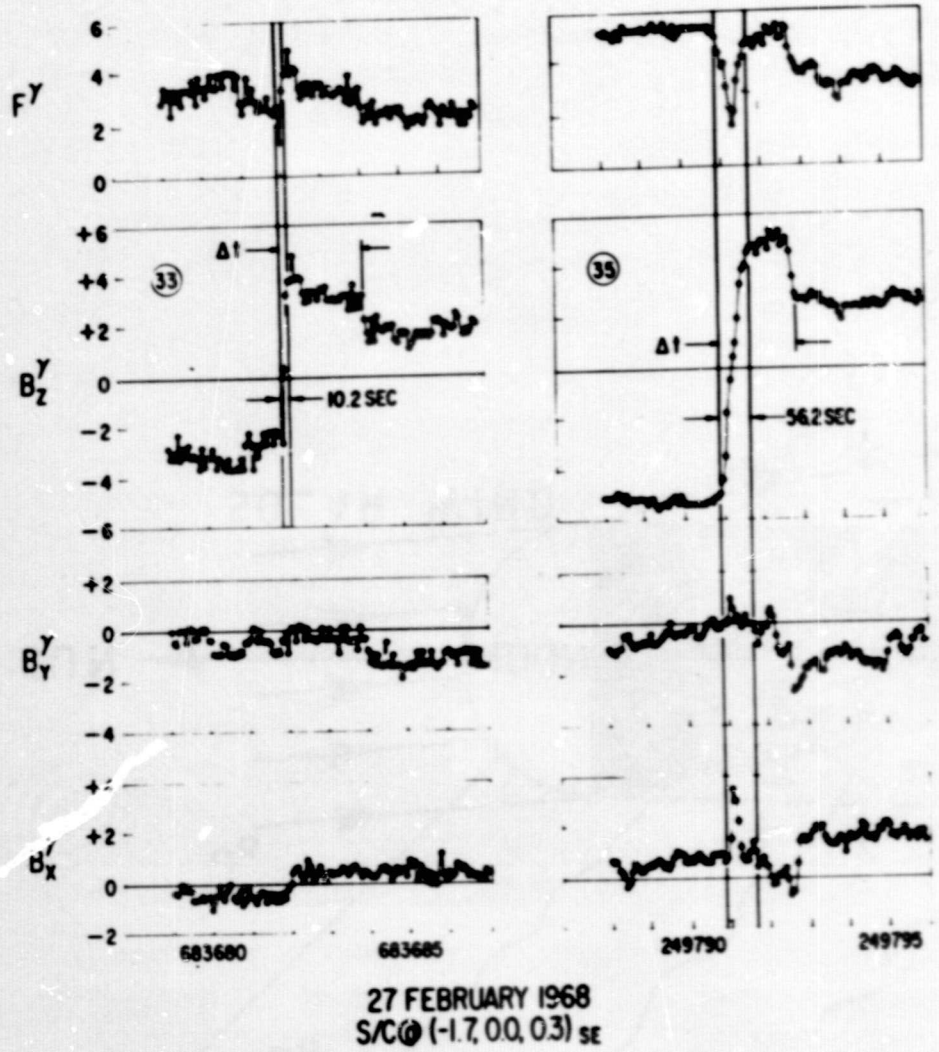
F^Y
B_Z^Y
B_Y^Y
B_X^Y
Δt
10.2 SEC
56.2 SEC
33
35
683680
683685
249790
249795
27 FEBRUARY 1968
S/C @ (-1.7, 0.0, 0.3) SE

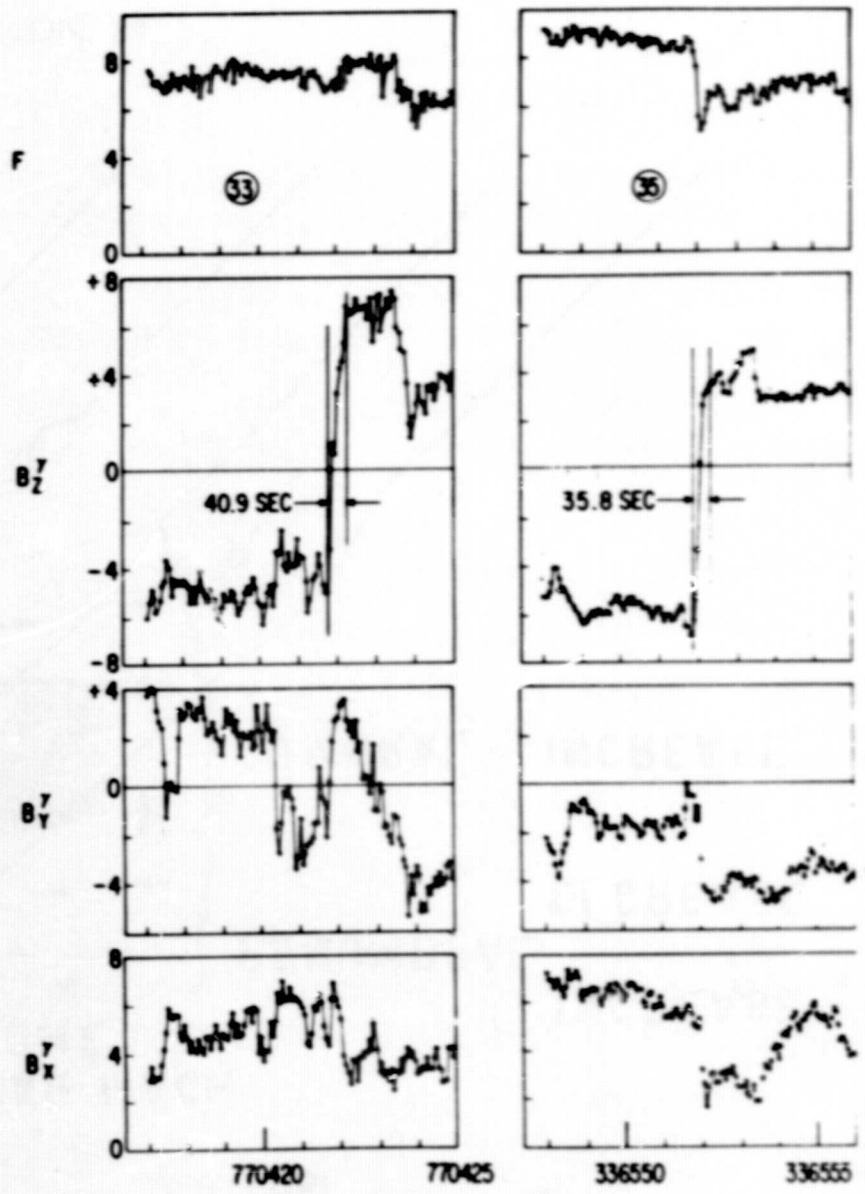
F
B_Z^Y
B_Y^Y
B_X^Y
40.9 SEC
35.8 SEC
33
35
770420
770425
336550
336555
19 MAY 1968
S/C AT (-1.3, 0.7, 0.0) SSE

FIGURE 23

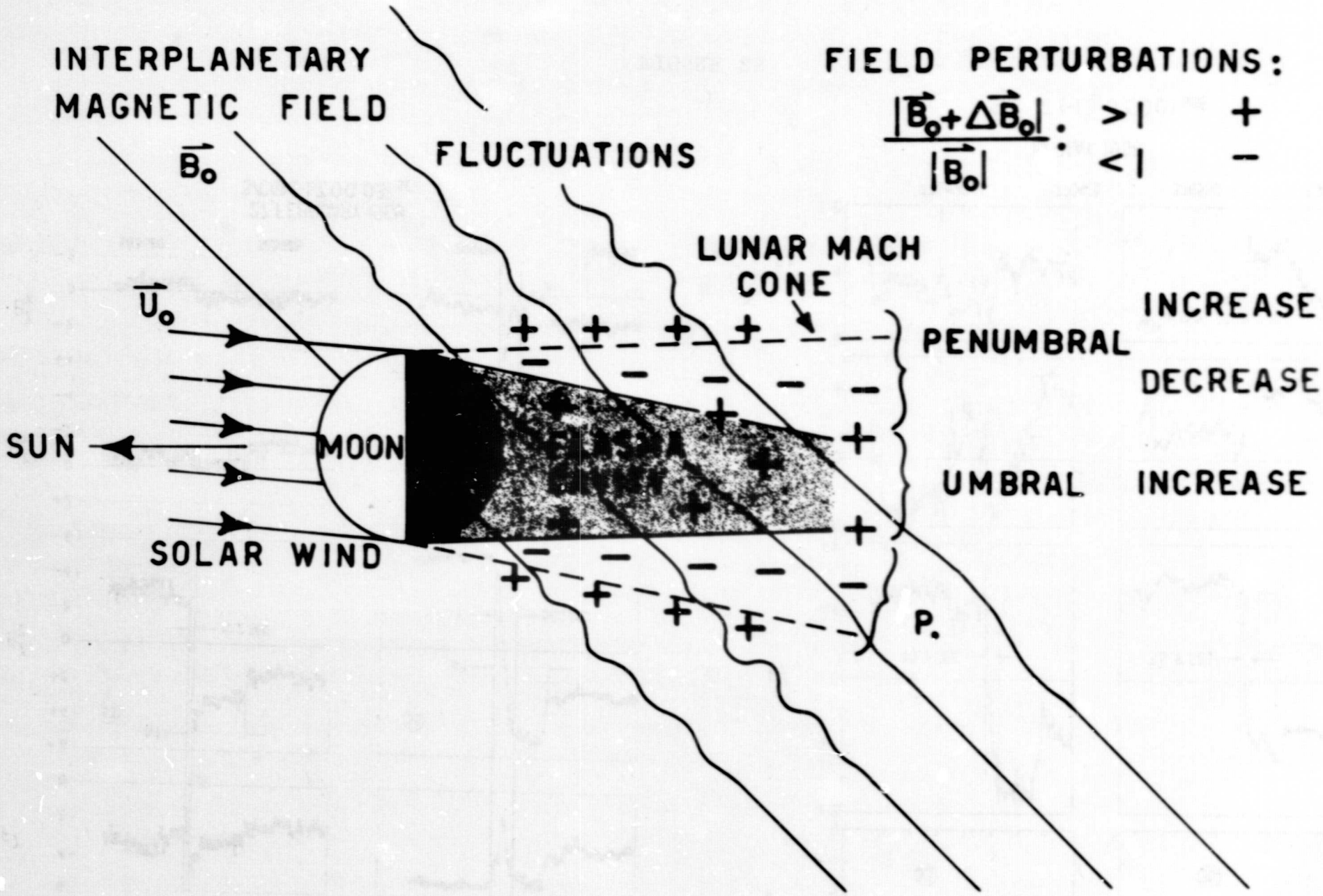
INTERPLANETARY
MAGNETIC FIELD
$\vec{B}_o$
FLUCTUATIONS
FIELD PERTURBATIONS:
$\frac{|\vec{B}_o+\Delta\vec{B}_o|}{|\vec{B}_o|}$: >1 +
<1 −
LUNAR MACH
CONE
$\vec{U}_o$
INCREASE
PENUMBRAL
DECREASE
SUN
MOON
UMBRAL INCREASE
SOLAR WIND
P.

FIGURE 24